

The PPG Physiological Signal for Heart Rate Variability Analysis

Gwo-Jia Jong¹ · Aripriharta¹ · Gwo-Jiun Horng²

Published online: 8 August 2017
© Springer Science+Business Media, LLC 2017

Abstract The photoplethysmography (PPG) sensor can be applied to measure the situation and function of human blood circulation. The PPG sensor is not only existed the characteristics of simple, convenient and low price but also easy non-invasive to measure physiological signal. The advantage of PPG signal is easy to measure from various sensing location. The physiological information of the clinical detection method is broadly implemented for such type. In this paper, we utilize “the green LED reflective” PPG sensor to capture physiological signals operated in static and exercise modes. Therefore, we adopted the short-term measurement in 5 min. Those captured signals are divided into five segments and 1 min for each segment. We calculated heart beats per minute and heart rate variability (HRV) operated in time domain analysis criteria. The related theory of short-time Fourier transform (STFT) combined with power spectral density (PSD) is implemented for finding HRV in frequency domain analysis. Then, we derived random process theory and the autocorrelation function which are verified the PPG measurement is stationary process or not. In the future experiment, we can compare the 24 h data with the previous results. Consequently, we apply the physical health status monitoring of long-term and short-term modes to observe subject varies of HRV and ANS after listening music concurrently.

Keywords PPG · STFT · PSD · HRV · ANS

✉ Gwo-Jiun Horng
grojjium@gmail.com

¹ Institute of Electronic Engineering, National Kaohsiung University of Applied Sciences, Kaohsiung City, Taiwan

² Department of Computer Science and Information Engineering, Southern Taiwan University of Science and Technology, Tainan City, Taiwan

1 Introduction

Recently, signal detection has become extensively important as they are used to assess the health of the lungs, heart and other parts of body under observation. Besides that, non-invasive methods using PPG signals have also gained significant attention by researchers.

The HRV analysis gives significant information on ANS's regulating function and balance status. HRV can be assessed in two ways, either as a time domain analysis or in the frequency domain as a PSD analysis. HRV is traditionally determined by digital processing of electrocardiograms (ECG). The R-wave peaks of QRS complexes in ECGs are detected by computer algorithms and R–R intervals (RRI) are calculated. Then, HRV parameters are computed using time domain and frequency domain methods [6].

However, the traditional measurement of ECG has several limitations: (1) ECG instruments generally require three electrodes attached to specific anatomical positions, which limit the subjects activities and make them uncomfortable; (2) the electrodes may cause skin irritations for some special subjects with allergies; (3) the ECG instruments are usually operated by specially trained nurses in the hospital and are not suitable for daily use at home. Therefore, new technologies have been developed to measure HRV without ECG, such as PPG [22].

In this paper, the green LED reflective PPG sensor is utilized to capture physiological signals. The main objective of our experiment is to understand various PPG signals in physiological state. Therefore, test status is divided into two parts: (1) static mode and (2) exercise mode.

In order to collect the signals, we adopt the short-term measurement in 5 min. In short, the main contributions of this paper are listed as follow: (1) We conduct the extensive experiment to capture the PPG signal from author only during static and exercise modes; (2) Before HRV analysis, normalized and smoothing process signals by using LabVIEW; (3) In time domain analysis, the 5 min length of HRV signal is divided into five groups, each 1 min for each group. Then, we calculated the heartbeat, SDNN, NN50, pNN50, nLF, nHF and LF/HF for each minute; (4) By using STFT in frequency domain analysis to observe the relative intensity of each band generated varies with time in time–frequency analysis diagram; (5) Using the concept of STFT which took time to cut a few part of signals, then the Fourier transform for each segment. We can get LF and HF values by PSD; (6) According to the static and exercise modes time and frequency domain results, we verify the measurement is stationary by favoring the autocorrelation coefficient and random procedure.

We adopted Pulse Sensor to observe physiological signals. So, the input is PPG signal. We investigated PPG signal for HRV using different physiological conditions. The rest of this paper has the following organization. Section 2 discusses related research on the Sect. 3 problem. Section 3 describes how to analysis PPG signal in time domain and frequency domain, introduced in this paper used STFT and person correlation coefficient. We showed experimental results in time domain and frequency domain and used correlation coefficient to analysis signals in Sect. 4. Section 5 discusses the conclusions and future work are mentioned for the progressing description.

2 Background Overview

2.1 Photoplethysmography

PPG are commonly worn on the fingertip. The purpose of using PPG is obtained PPI, and analysis time domain and frequency domain. PPG is the electro-optic technique of

measuring the cardiovascular pulse wave found in the human body. With every pulse the blood vessels increase in thickness and the body absorb more light, as the light have to travel through more tissue. The change in blood volume is synchronous to the heart beat, so it can be used to detect heart rate. Photoplethysmography is just a means of plethysmography that utilizes optical techniques.

The PPG measurement is entirely non-invasive and can be applied to any blood bearing tissue. In this paper, through light reflection measurement to measure PPG heartbeat is shown in the Fig. 1 [12].

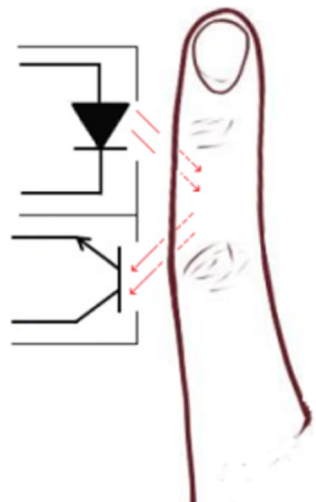
The PPG signals are commonly used in medical diagnosis to obtain vital physiological information. PPG signals are recorded and analyzed by PPG sensor to provide heart rate measurements. We can see the body's physiological data from the waveform of the PPG.

Optical sensors consist of a light source, typically a light-emitting diode, and a photodetector element. The light source is used to illuminate a region of tissue and the photodetector measures the amount of light exiting the tissue at a different location.

PPG signal composed by the two parts: (1) systolic, (2) diastolic. When the heart contraction, the pressure within the blood vessels, the blood volume of the generation period will continuously changed. If the heart diastolic pressure is relatively small, then the output of the previous systole blood circulation generated the impact of heart valve reflexed phenomenon, as shown in Fig. 2 [3, 4]. Thus, a complete PPG waveform includes the combination effects of systole pressure in the vessel wall. In addition, PPG will also be affected by the autonomic nervous system and the vascular status.

Currently, the most commonly used method is the optical detection. We use vascular caliber changes, reflecting the projected light, then through these angles to calculate continuous variation waveform vascular diameter. Detection principle of reflective optical sensors is shown in Fig. 3 [3, 4]. The LED light penetrate source into the skin, the light travel through the biological tissue, then the signal received by the photo detector. It used for measuring physiological signals to achieve the goal of non-invasive measurement. Optical measurement also can avoid signal interference of human potential and external signal to improve the accuracy of measurement. Therefore, light detection principle considerable number of applications in biomedical measurement.

Fig. 1 Schematic picture of reflection PPG [12]



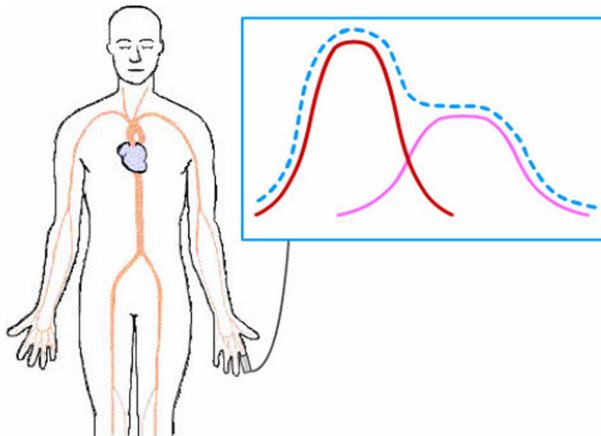


Fig. 2 PPG signal waveform diagram [3, 4]

The reflective PPG sensors have different light sources. The green LED is mainly used for sensing the heartbeat. The red and infrared LED light sources are used different light sources penetration intensities to compare, and calculate the oxygen concentration. Skin tissue and fat have a good absorption coefficient in green wavelength. Therefore, green light is more clearly observe heartbeat caused by the light intensity attenuation. We adopted the Pulse Sensor created by Joel Murphy and Yury Gitmanvanme as the heart rate sensor in this paper.

In Fig. 4, it is used to measure the pulse of the heart rate reflective photoelectric sensor. The Pulse Sensor uses PPG technology to generate the heartbeat signal. The small dimension and rounded shape of the Pulse Sensor makes it easy for capturing the heart rate signal from subject s' fingers. Moreover, Pulse Sensor is relatively energy efficient, using 3–5 V with current consumption around 4 mA at 5 V.

In Fig. 5, this sensor uses a green LED from Kingbright (AM2520ZGC09) to illuminate the subject's fingertip, and a light photo sensor from Avago (APDS-9008) measures the amount of light reflected back from the fingertips [5].

By using the datasheet of AM2520ZGC09 [9] and APDS-9008 [10], the green LED generates light around 500 nm. The light sensor is extremely sensitive to detect light of the same wavelength. Moreover, the light producer and sensor are perfectly matched, allowing them to work together to effectively measure heart beat waveforms. Because of the green

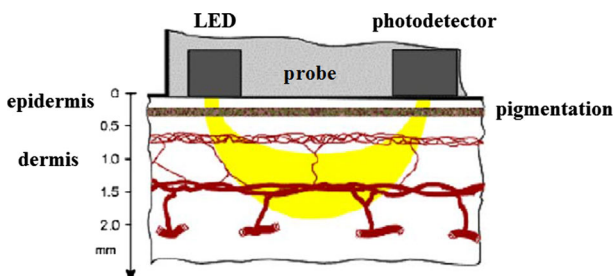


Fig. 3 Reflective optical sensor [2, 3]

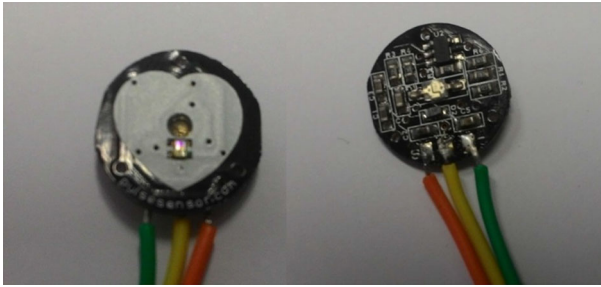


Fig. 4 Appearance of the pulse sensor



Fig. 5 Block diagram of the pulse sensor

wavelength of 500 nm, it is not possible to use this sensor for measuring blood oxygen concentration.

It uses a low-pass filter and MCP6001 [11] amplifiers in the back of the sensor, the amplified signal 330 times. Therefore, amplified signal can be easily collected.

In this paper, we used Pulse Sensor to collect subject's physiological data, and then calculate the subject's physiological state through LabVIEW.

2.2 Blood Pressure (BP)

BP is the pressure exerted by circulating blood upon the walls of blood vessels, and is one of the principal vital signs. Blood pressure usually refers to the arterial pressure of the systemic circulation. During each heartbeat, blood pressure varies between a maximum (systolic) and a minimum (diastolic) pressure. The blood pressure in the circulation is principally due to the pumping action of the heart. A normal blood pressure should be around 120/80 to be accounted for as a safe level, with 120 being measured through systole, and 80 through diastole [6].

In modern medicine, different physiological parameters have been widely used in the prevention of various diseases, as well as the initial detection of disease, wherein the blood pressure parameters used to evaluate the probability of the cardiovascular disease occur.

The Mean Arterial Pressure (MAP) is derived from a patient's Systolic Blood Pressure (SBP) and Diastolic Blood Pressure (DBP). According to DBP, SBP and MAP, the blood pressure can be a basis to diagnosis health of patient. The detail of DBP and SBP is shown in Table 1 [25]. The MAP should be calculated when the clinical scenario mandates a blood pressure adjustment based on MAP rather than SBP, as well as for the management of patients with acute conditions, where there is a concern for appropriate organ perfusion. The relativity between blood pressure and heart as described follows:

$$MAP = DBP + \frac{1}{3} \times (SBP - DBP) \quad (2.1)$$

Blood pressure is measured in millimeters of mercury (mm Hg). The higher number indicates systolic blood pressure. The lower number is diastolic blood pressure.

In Fig. 6 [23], the diastolic pressure is the relaxation of the chambers of the heart whereas systole is the contraction of the heart chambers. Therefore, the systolic pressure will show the pressure that your heart emits when blood is forced out of the heart, while diastolic pressure is the pressure exerted when the heart is relaxed. This is the main mechanism by which blood pressure operates [7].

American Heart Association (AHA) defined BP as 120/80 and (90–119)/(60–79) for the ideal blood pressure. The 115/75 is the best blood pressure. Currently, the high, low and normal blood pressure ranges are shown in Table 2 [8]. Table 3 [18] is a reference for you regarding the normal blood pressure level for 1–64 years old elderly. Different gender and age shows different ranges. Most people are not living in the ideal of healthy lifestyle and life continue to rise in blood pressure.

2.3 Heart Rate Variability

HRV has emerged as multidisciplinary areas of research mainly due to continuous interactions between engineers, physicians and physiologists [17]. The parameter of HRV is important physiological information. In this paper, the HRV is an important basis of analysis in the PPL.

The HRV analysis gives significant information on Autonomic Nervous System (ANS)'s regulating function and balance status. The variation of heart rate during short

Table 1 Features of systolic and diastolic [25]

Indicator	Diastolic	Systolic
Definition	It is the pressure that is exerted on the walls of the various arteries around the body in between heart beats when the heart is relaxed	It measures the amount of pressure that blood exerts on arteries and vessels while the heart is beating
Normal range	60–80 mmHg (adults); 65 mmHg (infants); 65 mmHg (6–9 years)	90–120 mmHg (adults); 95 mmHg (infants); 100 mmHg (6–9 years)
Importance with age	Diastolic readings are particularly important in monitoring blood pressure in younger individuals	As a person's age increases, so does the importance of their systolic blood pressure measurement
Blood pressure	Diastolic represents the minimum pressure in the arteries	Systolic represents the maximum pressure exerted on the arteries
Ventricles of the heart	Fill with blood	Left ventricles contract
Blood vessels	Relaxed	Contracted
Blood pressure reading	The lower number is diastolic pressure	The higher number is systolic pressure
Etymology	"Diastolic" comes from the Greek diastole meaning "a drawing apart"	"Systolic" comes from the Greek systole meaning "a drawing together or a contraction"

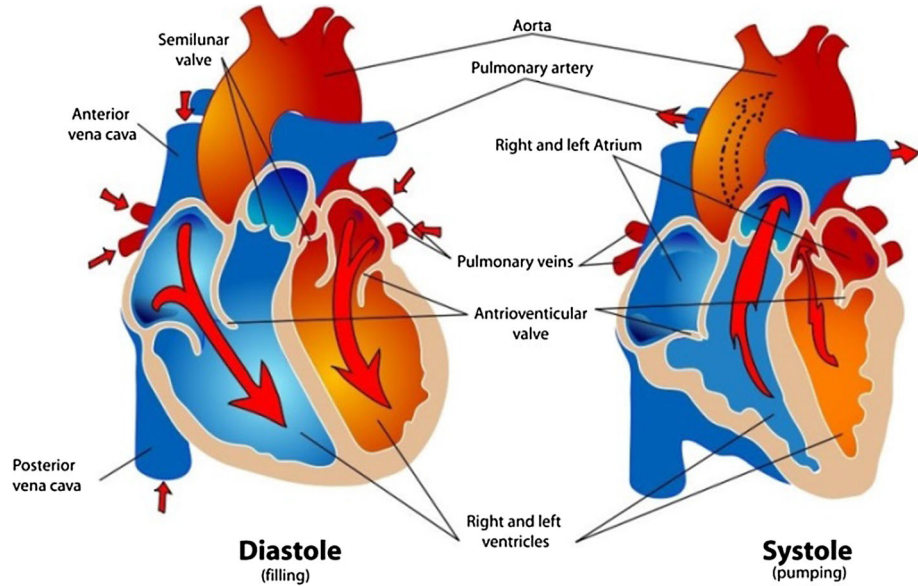


Fig. 6 Systolic and diastolic of heart activity [23]

Table 2 Range of systolic and diastolic [8]

Status	Systolic	Diastolic
Hypotension	<90	<60
Desired blood pressure	90–119	60–79
Prehypertension	120–139	80–89
Stage 1 Hypertension	140–159	90–99
Stage 2 Hypertension	160–179	100–109
Hypertensive crisis	≥180	≥110

term is analyzed with the method of time domain and frequency domain to provide the degree of balance and activity of ANS.

Heart rate variability, or HRV for short, is the degree of fluctuation in the length of the intervals between heartbeats [16]. The physiological origins of HRV are the fluctuations of the activity of cardiovascular vasoconstriction and vasodilation centers in brain. Normally, these fluctuations are a result of blood pressure oscillation, respiration, thermoregulation and circadian biorhythm.

As shown in Fig. 7, R–R intervals (RRI) or P–P intervals (PPI) can influence the length of beat-to-beat intervals and are measured in millisecond (ms). R–R intervals or P–P intervals are obtained from ECG or plethysmography [19]. The analysis method includes time domain analysis and frequency domain analysis, as shown in Fig. 8.

HRV can be assessed in two ways, either as a time domain analysis or in the frequency domain as a Power Spectral Density (PSD) analysis. In either method, the time intervals between each successive normal P–P interval (PPI) are first determined. The most important time domain measures are the SDNN, SDNN Index and the R-MSSD. The item of time domain is shown in Table 4 [2, 15].

Table 3 Features of SBP and DBP [18]

Gender	Age	N	SBP (mmHg)		DBP (mmHg)	
			Average	SD	Average	SD
Male	1–6	464	96.3	11.2	57.3	12.1
	7–12	987	105	11.9	65.2	11.9
	13–18	952	117.7	12.9	69.9	12.2
	19–44	988	121.2	13.3	78.3	12.3
	45–64	960	131.1	20.2	84.4	12.7
	≥65	485	137.8	20.2	79	12.6
	≥19	2433	125.4	17.1	79.8	12.7
	≥45	1445	133.3	20.5	82.6	12.9
Female	1–6	466	94	9.9	56.7	10.6
	7–12	988	104.8	12.1	64.3	11.5
	13–18	959	109.6	10.6	68.7	11.3
	19–44	1013	110.7	12.9	71.8	11.9
	45–64	961	128	19.7	81.1	11.2
	≥65	486	145	23.2	79.6	14.2
	≥19	2460	118.3	19.7	74.8	12.7
	≥45	1447	133	22.2	80.6	12.1

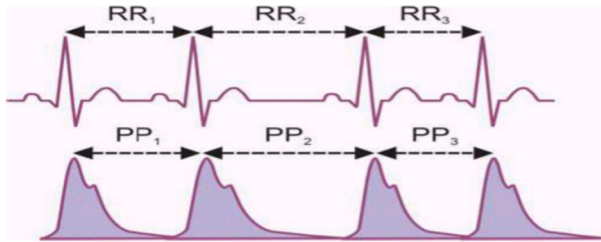


Fig. 7 HRV standard of each band [19]

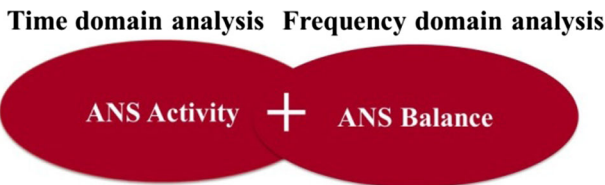


Fig. 8 Time–frequency domain analysis

HRV measurements differentiate 24 h long-term recordings and short-term 5 min recordings by statistical variables analysis. The frequency domain is suitable for short-term analysis. HRV was measured with the power spectral analysis by Hyndman and Gregory in 1975. In the frequency domain HRV measurement are based on the PSD of the R–R interval or P–P interval calculated. The PSD is analyzed by calculating power and peak frequency for different frequency bands. [23].

Table 4 Time domain analysis of HRV [2, 15]

Indicator	Description	Unit
SDNN	SD of all normal to normal intervals	ms
SDANN index	SD of the averages of NN intervals in all 5 min segments of the entire recording	ms
SDNN index	Mean of the SDs of all NN intervals for all 5 min segments of the entire recording	ms
R-MSSD	The square root of the mean of the sum of the squares of differences between adjacent NN intervals	ms
NN50	Number of pairs of adjacent NN intervals differing by more than 50 ms in the entire recording	%
pNN50	The ratio of a complete RR wave that the interval time is over 50 ms	None

The commonly used frequency (VLF, 0.003–0.04 Hz), low frequency (LF, 0.04–0.1 Hz), high frequency (HF, 0.15–0.4 Hz), include value of LF/HF, and total power (TP). The standard of each band is shown in Fig. 9 [15]. The power of LF and HF order control and balance of sympathetic and parasympathetic to normalize, which is relative value with assessment of the LF and HF power to total power. The item of frequency domain analysis is shown in Table 5 [2].

3 Methodology

We explained how to measure and analyze subject's data in the time domain and frequency domain. We utilized Pulse Sensor display in Fig. 10 to measure PPI of PPG signals. In the experiment, six subjects were recorded during 5 min in static and dynamic conditions.

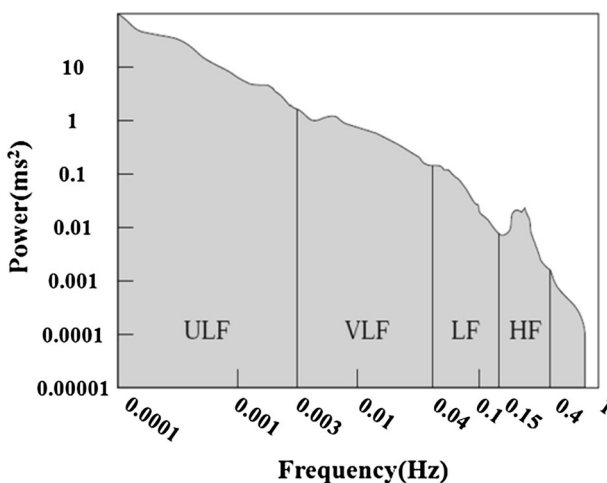
**Fig. 9** HRV standard of each band [15]

Table 5 Frequency domain analysis of HRV [2]

Indicator	Description	Unit
TP	Frequency domain of HRV	ms ²
LF	Power in the low frequency range	ms ²
LF norm	LF power in normalized units	None
HF	Power in high frequency range	ms ²
HF norm	HF power in normalized units	None
LF/HF	Value of LF/HF	None

By utilizing USB-6009 developed by National Instruments to measure Pulse Sensor's output signal as shown in Fig. 11. We adopt USB-6009 to measure PPG signal in differential input mode, and set the sample rate is 100 Hz shown as Fig. 12.

And then, we analyzed signals which recorded 5 min through LabVIEW. The procedure of HRV analysis is shown as Fig. 13. The HRV is calculated by PPI and heart rate. The main analysis of heartrate is normal heart beat research.

3.1 Time–Frequency Domain Measurement and Analysis

Figure 14 shows the raw data for 5 min which recorded by Pulse Sensor. By favoring LabVIEW, we process those data. Figure 15 shows flow diagram of the signals analysis. In the section, we explained how to analyze signals in time domain and frequency domain.

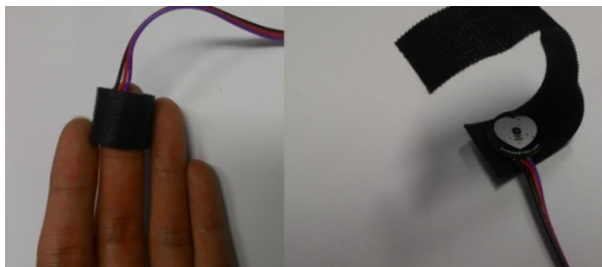
In order to do signal processing in LabVIEW, we first normalized the raw data from Pulse Sensor. The normalized signal is shown in Fig. 16.

The second step is signal smoothing. In this paper, we demonstrated the smoothing process: (1) before and (2) after. The objective of signal smoothing is to reduce the impact of noise in HRV measurement. In Fig. 17, we can show the signal before smoothing. Figure 18 displays the signal after smoothing process.

In third step, we could find heart rate and the parameters of heart rate variability in time domain. Furthermore, there are two ways to calculate heartbeats; one is to be calculated by (3.1).

$$\text{Heart rate} = \frac{1}{PPI} \times 60(\text{bpm}) \quad (3.1)$$

The other method is to find the waveform produced in 1 min, and then calculate the peaks of each waveform shown as Fig. 19.

**Fig. 10** Pulse sensor

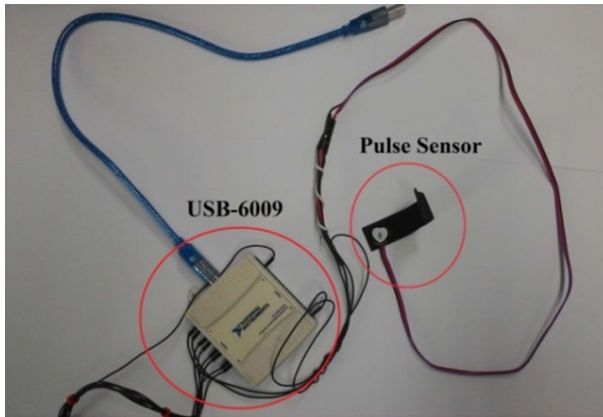


Fig. 11 Pulse sensor plugged into USB-6009

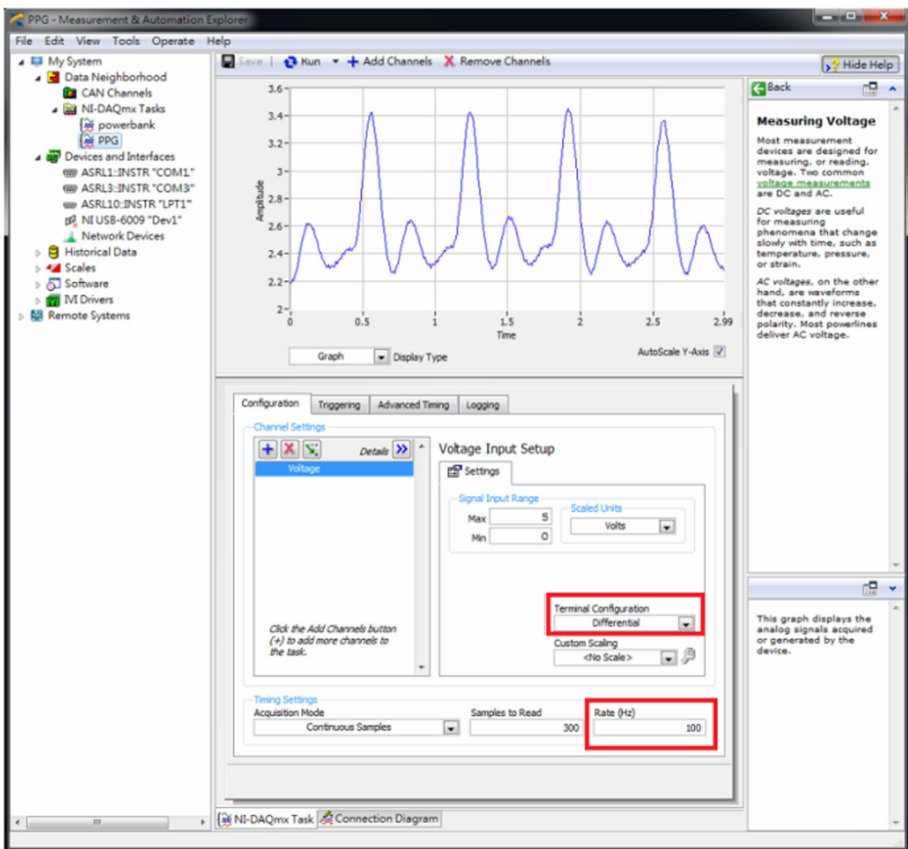


Fig. 12 Sample rate setting

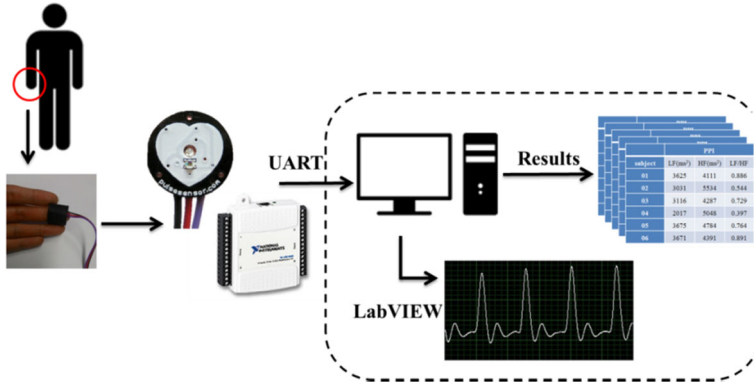


Fig. 13 HRV analysis step

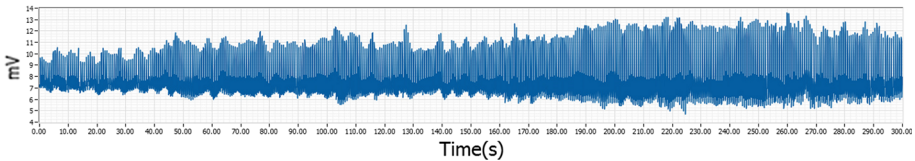


Fig. 14 The output signal from pulse sensor

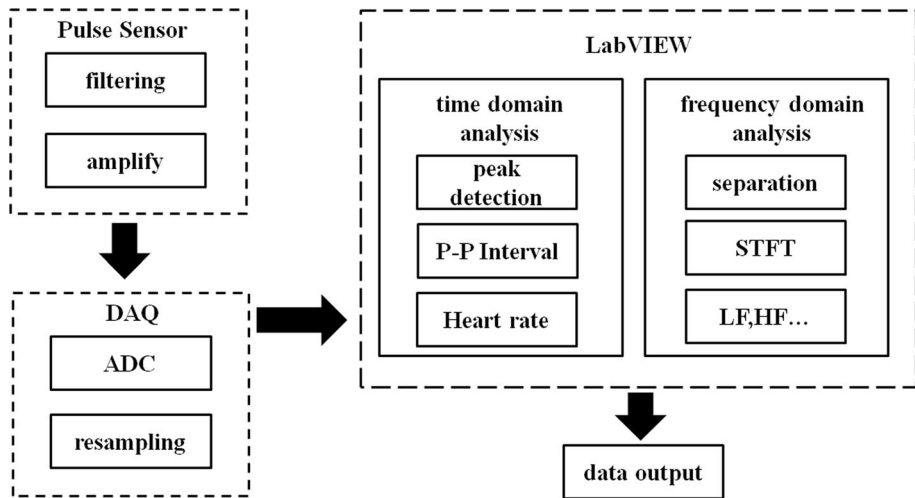


Fig. 15 Flow diagram of the signals analysis

The 5 min length signal is divided into five groups, 1 min for each group. Then, the heart beats calculate for each minute as shown in Fig. 20.

Clinically, SDNN is the most commonly used to make recommendations heart rate variability index in time domain analysis. In Kleiger's paper [24], SDNN can be predicted death after myocardial infarction, is independent of the known risk factors such as left ventricular output rate (LVEF) or ventricular arrhythmia.

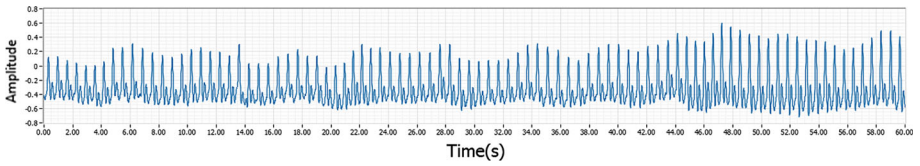


Fig. 16 Normalization signal

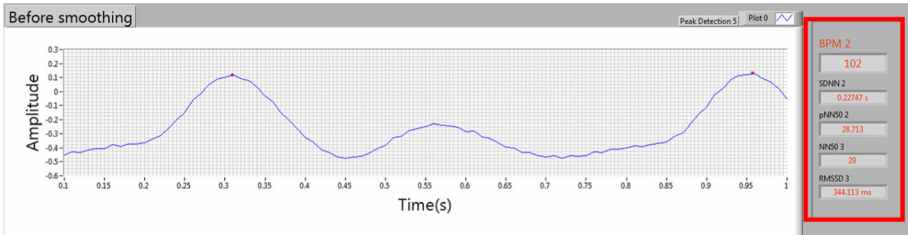


Fig. 17 Signal before smoothing

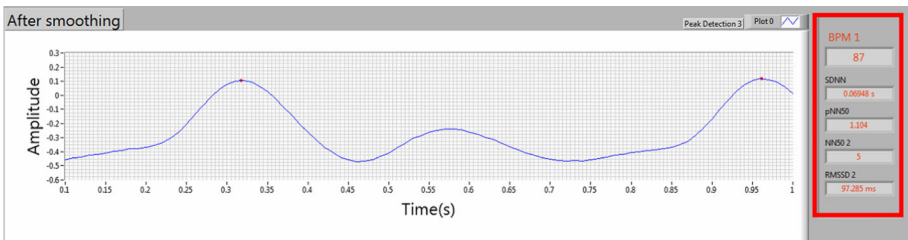


Fig. 18 Signal after smoothing

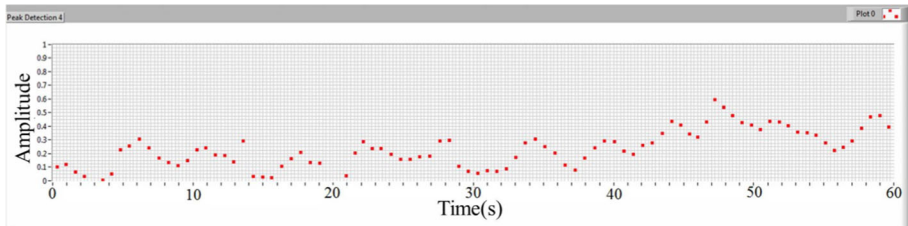


Fig. 19 Peak detection and calculate heart beats

In this paper, we used recorded 5 min signals, and LabVIEW to design a high-pass filter. The threshold value for high pass filter should be entered to find P points. Then, we calculate the value of P–P interval through LabVIEW design program. After got the value of P–P interval, we use LabVIEW’s HRV Analysis VI to calculate SDNN as following [20]:

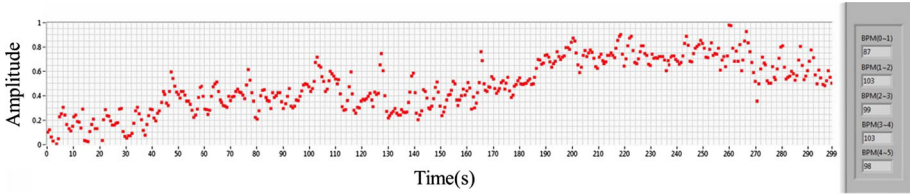


Fig. 20 Calculate heart beats in each minute

- Mean PP

$$\text{Mean} = \frac{\sum_{i=1}^n P_i}{n} \tag{3.2}$$

where P_i is P–P interval (PPI) in millisecond.

- SDNN (Standard deviation of normal interval):

The parameter represent heart rate variability of total, because SDNN average same with total power.

$$\text{SDNN} = \sqrt{\sum_{i=1}^n \frac{1}{n} (P_i - \bar{x})^2} \tag{3.3}$$

where \bar{x} is the value of PPI average.

- RMSSD (The root mean square of successive differences between adjacent NN interval):

RMSSD represent Parasympathetic activity, if RMSSD less than 20 of Parasympathetic Decreased ability to regulate for heart.

$$\text{RMSSD} = \sqrt{\sum_{i=2}^n \frac{1}{n-1} (P_i - P_{i-1})^2} \tag{3.4}$$

We want to know PPG waveforms in the frequency domain, so we used short-time Fourier transform (STFT) for analysis. In STFT’s time–frequency analysis diagram, it can be seen that the frequency distribution for each time shown as Fig. 21.

We can observe the relative intensity of each band generated varies with time in time–frequency analysis diagram. But, it is difficult to see LF and HF values in time–frequency analysis diagram, so we used a different method to get LF and HF values. The concept of STFT which took time to cut a few part of signals, then the Fourier transform for each segment shown as Fig. 22 [13]. In our experiments’ case, we recorded signal for 5 min, and cut five segments, 1 min for each segment, then used FFT for each segment shown as Fig. 23.

We applied FFT for 5 min as shown in Fig. 24. In order to observe different between short time and direct FFT analysis, and the result of 5 min FFT analysis as shown in Fig. 24. Another point of view, STFT has a higher temporal resolution than FFT; it can help us understand the relative intensity of each band generated varies with time.

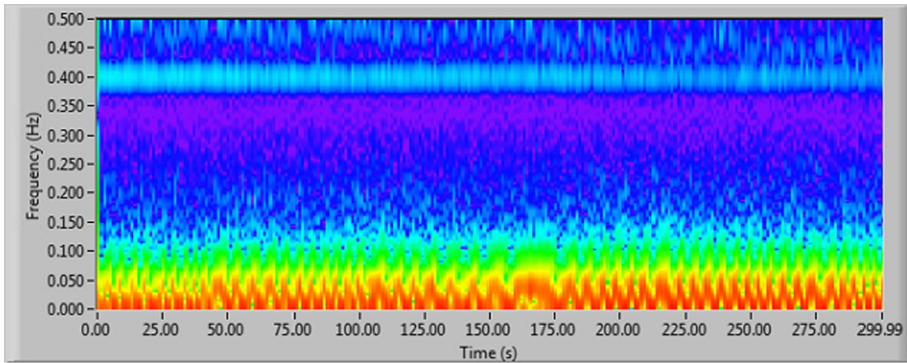


Fig. 21 Time versus frequency diagram

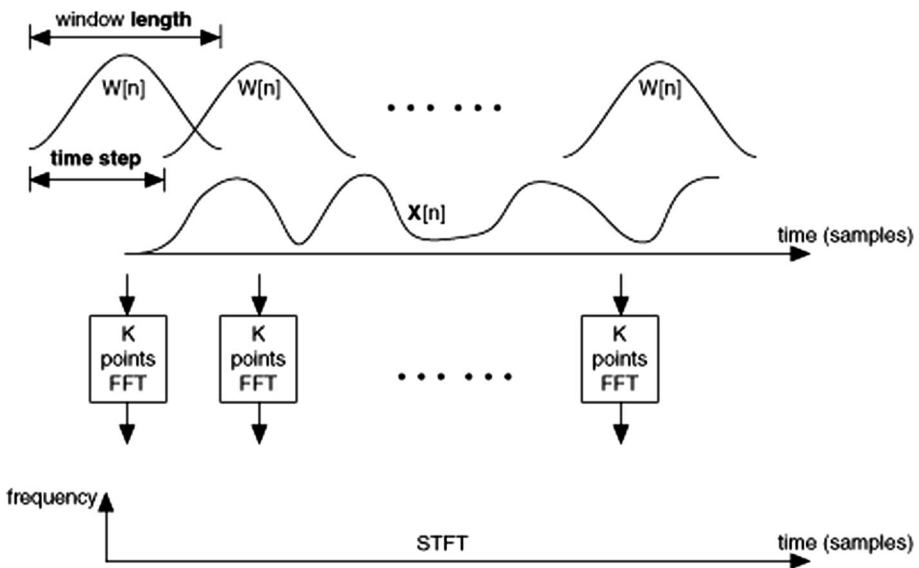


Fig. 22 Schematic diagram of STFT [13]

3.2 Short Time Fourier Transform

In this paper, we used STFT to observe the time and frequency variation in PPG waveforms. For signal or time series analysis, Fourier analysis provides several advantages: a simple way for us, enables us to analyze through Fourier method, and obtaining characteristics of signals, also further understanding of the physical meaning of signals implied.

Fourier analysis is the use of a complex sine wave signal $e^{i\omega t}$ as the basis function to complete transform; generally this conversion is defined as:

$$F(\omega) \leq f(t), e^{i\omega t} \geq \int f(t)e^{-i\omega t} dt \tag{3.5}$$

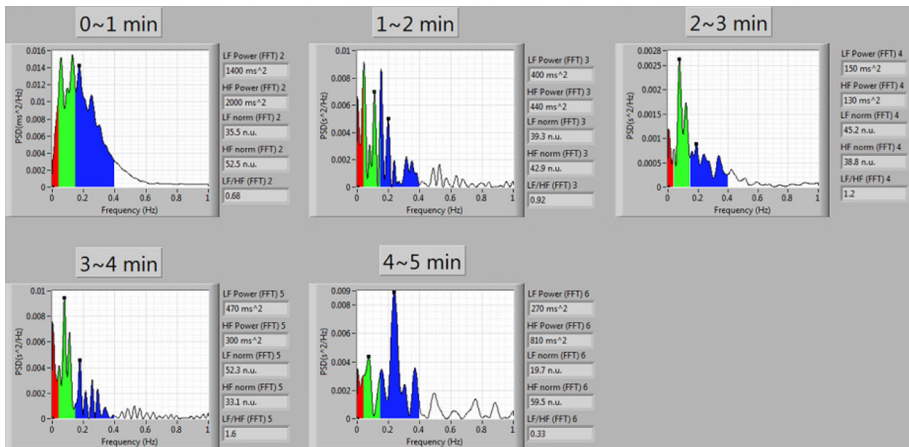


Fig. 23 FFT for each minute

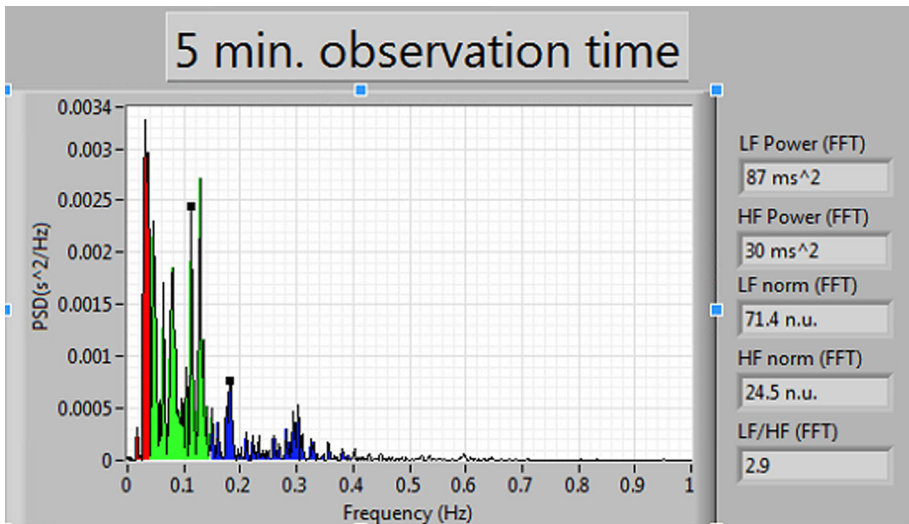


Fig. 24 FFT for 5 min

It is a linear combination of the signal into a number of fixed frequency harmonic functions; the size of each harmonic function is also representative of a certain frequency of the harmonic function with the energy magnitude, so we get frequency distribution of energy from Fourier analysis.

Because e^{icot} is an unlimited extension of the basal function on the time axis, so the message at any time-local spread to the whole of the frequency axis, it is difficult to distinguish these messages on $F(\omega)$. In order to be able clearly describe the information signal same time in the frequency and time area, STFT is proposed. STFT is a time-frequency representations analytical technique, which is defined as:

$$F(\tau, \omega) = \int f(t)w(t - \tau)e^{-i\omega t} dt \tag{3.6}$$

In which $w(\cdot)$ is some suitable window function (e.g., Gaussian). The STFT’s basis function is to do different frequency modulation and time shift to produce. But, STFT have a resolution limit problem. Due to the basic functions on each frequency modulation function has a window function which at the same time support width. So, the results the time–frequency resolutions at each position on plane are same, as shown in Fig. 25 [1].

In addition, according to the uncertainty principle:

$$\Delta t \Delta \omega \geq \frac{1}{2} \tag{3.7}$$

In which Δt is the base time to support the width; $\Delta \omega$ is base band width. This theorem prevents the substrate in the frequency or times have any resolution, this means that between the time and frequency have resolution trade-offs exist problems. Use a time to support narrow substrate, an increase of resolution in time, will reduce the frequency resolution. Similarly, it reduces the resolution in time and it increases the frequency resolution.

3.3 Pearson Correlation coefficient

In order to verify whether the value each time correlated, we used the correlation coefficient to analysis. The correlation coefficient between two variables is used to reflect the linear relationship between intensity and direction. The most commonly used is the Pearson product-moment correlation coefficient, which defined as two divided by two variable covariance standard deviation (the square root of the variance). The range of the correlation coefficient is $[-1, +1]$. The correlation coefficient for the “+1” represents that two groups of variables are perfect positive correlation. Meanwhile, “-1” represents two groups of variables perfect negative correlation. The formula of Pearson product-moment correlation coefficient is as following [14, 21]:

$$Corr = \frac{\sum_{i=1}^N (X_i - \bar{X})(Y_i - \bar{Y})}{\sqrt{\sum_{i=1}^N (X_i - \bar{X})^2} \sqrt{\sum_{i=1}^N (Y_i - \bar{Y})^2}} \tag{3.8}$$

We can see that the degree of correlation values through the Table 6.

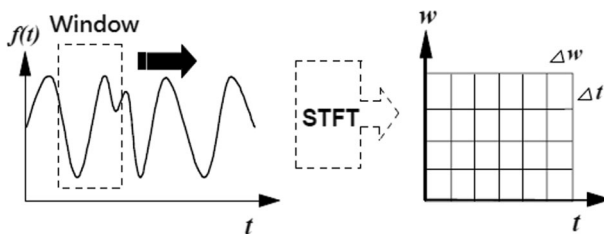


Fig. 25 Basic function of STFT in the time–frequency resolution [1]

Table 6 The absolute value of the correlation coefficient and relevance

The absolute value of the correlation coefficient	Relevance
$ r = 1$	Perfect correlated
0.7–0.99	Highly correlated
0.4–0.69	Moderately correlated
0.1–0.39	Modestly correlated
0.01–0.09	Weakly correlated
$ r = 0$	Uncorrelated

4 Experimental Results

4.1 Experimental Results

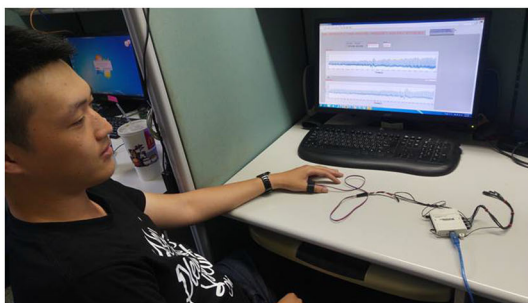
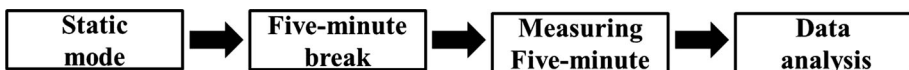
The main objective of our experiment is to understand differences PPG signals in physiological state. Test status is divided into two parts: (1) static mode (2) exercise mode. Static mode measurements were measured with the most comfortable position as shown Fig. 26. First, subject need to relax 5 min. After relaxing, we capture the PPG for 5 min by means of PPG sensor. The measurement values are store in LabVIEW and use for analysis.

The exercise mode measurements were measured after spinning 5 min shown as Fig. 27.

After the test, the signal processing and computing is done through LabVIEW. Finally, the computation of the heartbeat, SDNN, NN50, pNN50, nLF, nHF and LF/HF, and data through Excel for statistical analysis.

4.2 Static Mode Time Domain Analysis Results

The data were recorded 10 times. After signal normalized and smoothed, we used LabVIEW's HRV Analysis VI to calculate SDNN, NN50 and pNN50. The result for data analysis is shown in the Table 7.



Measuring five-minute in static mode

Fig. 26 Static mode measurement block diagram

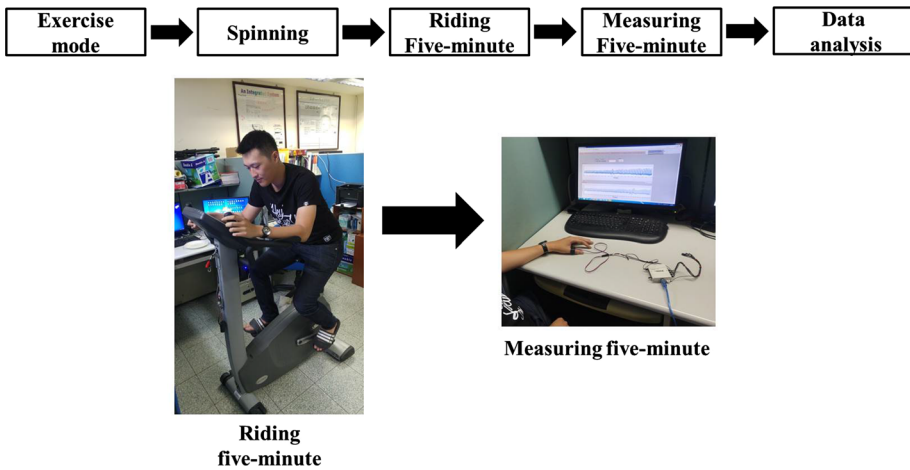


Fig. 27 Exercise mode measurement block diagram

4.3 Static Mode Frequency Domain Analysis Results

The next step is frequency domain analysis. We used two methods for frequency domain analysis of subject in static mode. The first method is directly transformed the whole recorded signal (Fig. 28) to see the frequency distribution. The results are shown in Fig. 29. The second method is FFT analysis for five groups separated recorded signal. Figure 30 shows the frequency distribution of each group. In addition, we also used FFT for comparing the 1 and 5 min length signals Figs. (31, 32, 33, 34, 35, 36, 37, 38, 39, 40, 41, 42, 43, 44, 45, 46, 47, 48, 49, 50, 51, 52, 53, 54, 55, 56, 57).

Table 7 Time domain results in static mode

Time period (min)	0–1	1–2	2–3	3–4	4–5	0–5		
	HR (bpm)	HR (bpm)	HR (bpm)	HR (bpm)	HR (bpm)	SDNN (ms)	NN50 (count)	pNN50 (%)
<i>Static mode</i>								
1	98	100	99	99	99	27.60	1	0.202
2	98	96	95	96	96	26.48	2	0.416
3	94	91	93	92	91	25.24	1	0.217
4	87	91	96	91	89	25.08	1	0.219
5	88	87	86	87	88	37.86	1	0.229
6	102	95	96	94	99	18.79	2	0.412
7	95	93	92	94	91	24.36	1	0.211
8	80	81	83	84	80	28.56	1	0.223
9	85	83	81	84	82	21.23	1	0.209
10	93	91	94	95	92	24.28	1	0.215

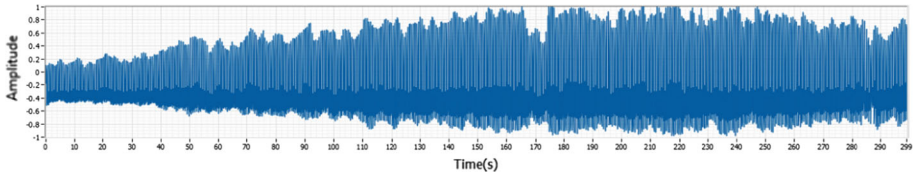


Fig. 28 Subject 1 signal in static mode

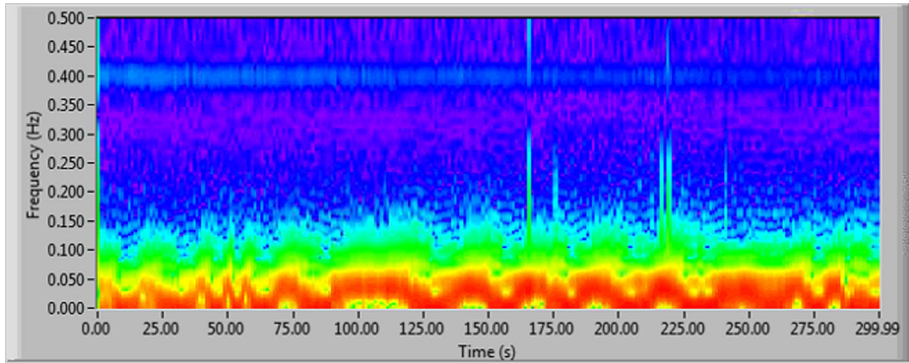


Fig. 29 Subject 1 result in static mode utilizing the STFT method

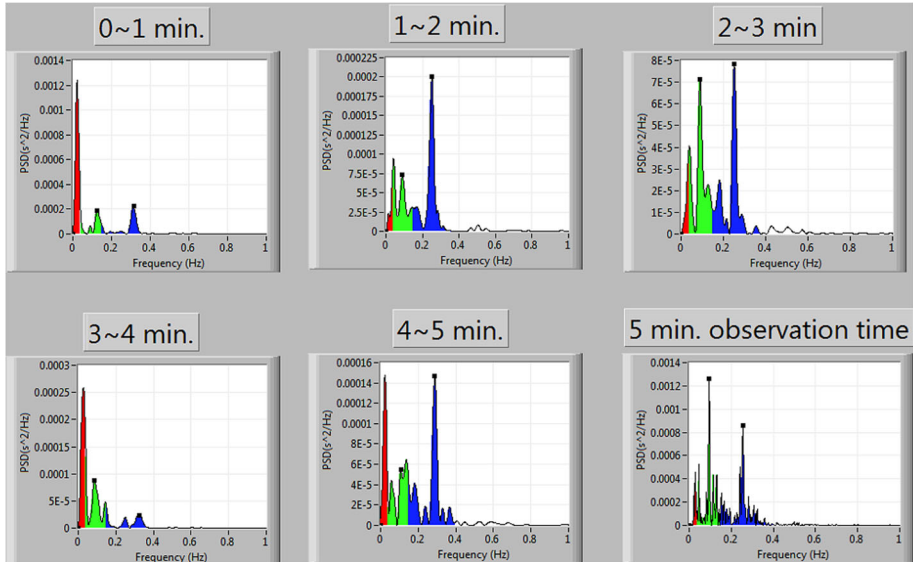


Fig. 30 Subject 1 result in static mode using the FFT method

We recorded ten times data in static mode, using STFT and FFT to analysis and find frequency distribution as LF, HF and LF/HF. Between Figs. 28 and 57 are frequency domain results in static mode. After frequency domain analyzed, we recorded results shown in Tables 8 and 9.

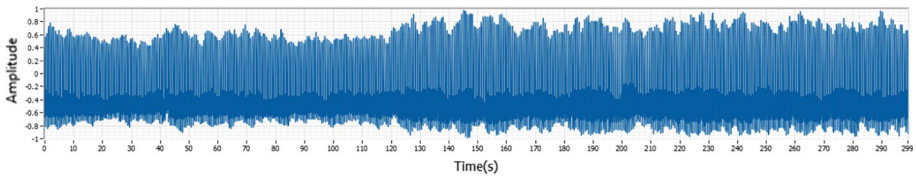


Fig. 31 Subject 2 signal in static mode

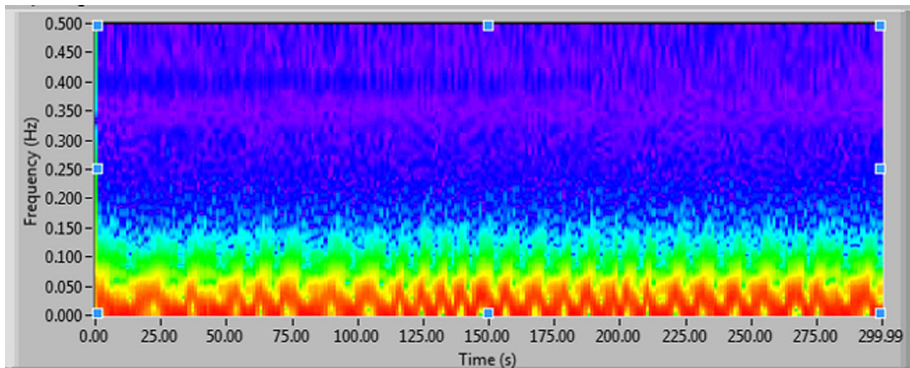


Fig. 32 Subject 2 result in static mode utilizing the STFT method

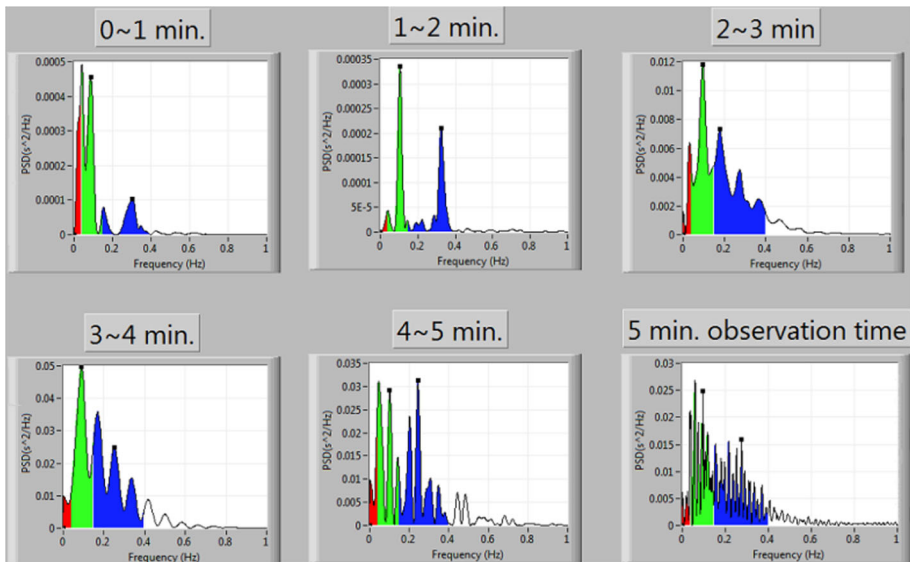


Fig. 33 Subject 2 result in static mode utilizing the FFT method

Tables 8 and 9 shows the recorded nLF, nHF and LF/HF for static mode. Time period was divided into 5 groups: 0–1, 1–2, 2–3, 3–4, and 4–5. In addition, the data derived from 5 subjects; namely subject 1 to subject 5. Table 9 shows the nLF, nHF and LF/HF values for

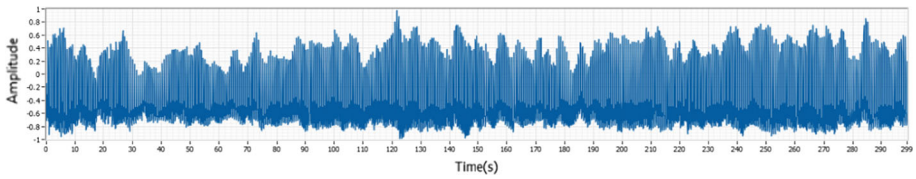


Fig. 34 Subject 3 signal in static mode

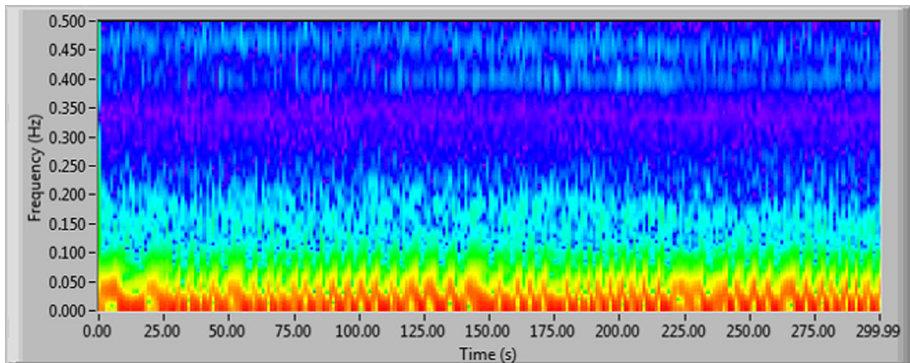


Fig. 35 Subject 3 result in static mode utilizing the STFT method

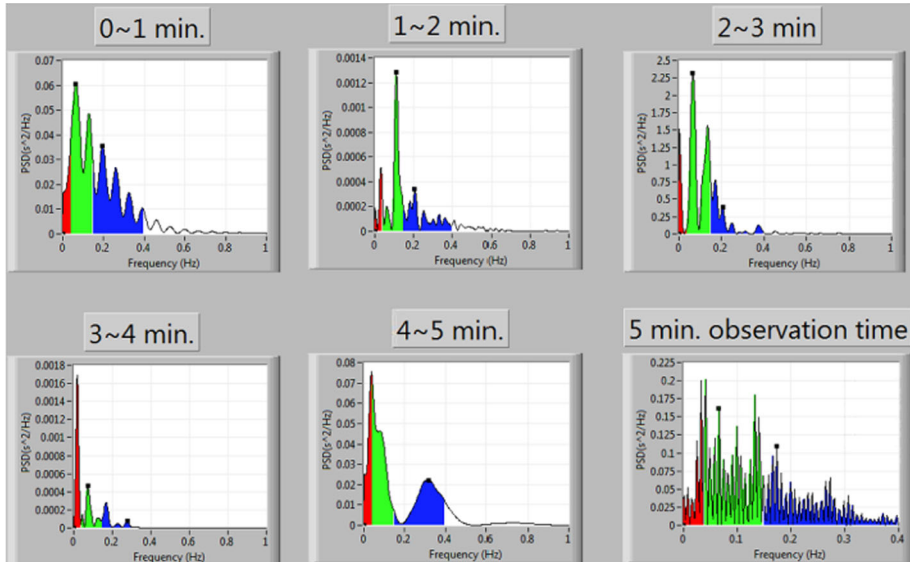


Fig. 36 Subject 3 result in static mode utilizing the FFT method

subject 6 to subject 10. We use Tables 8 and 9 to calculate the correlation coefficient as shown in Table 10. Table 11 shows the results of FFT transform which used the second method. Furthermore, the results show nLF, nHF and LF/HF from 10 subjects of experiment in static case.

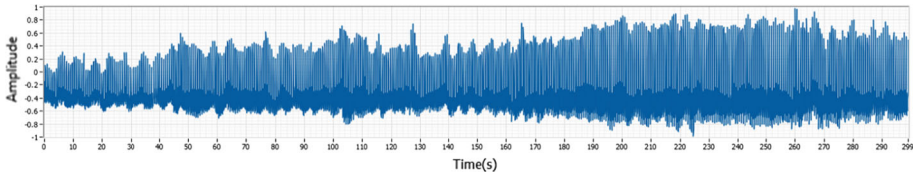


Fig. 37 Subject 4 signal in static mode

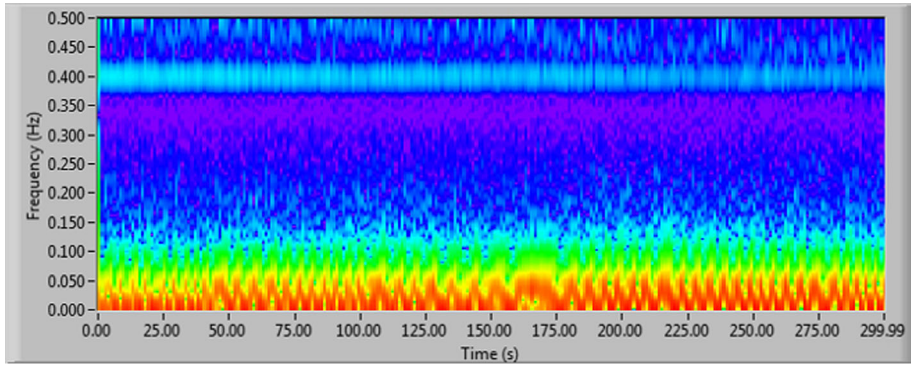


Fig. 38 Subject 4 result in static mode utilizing the STFT method

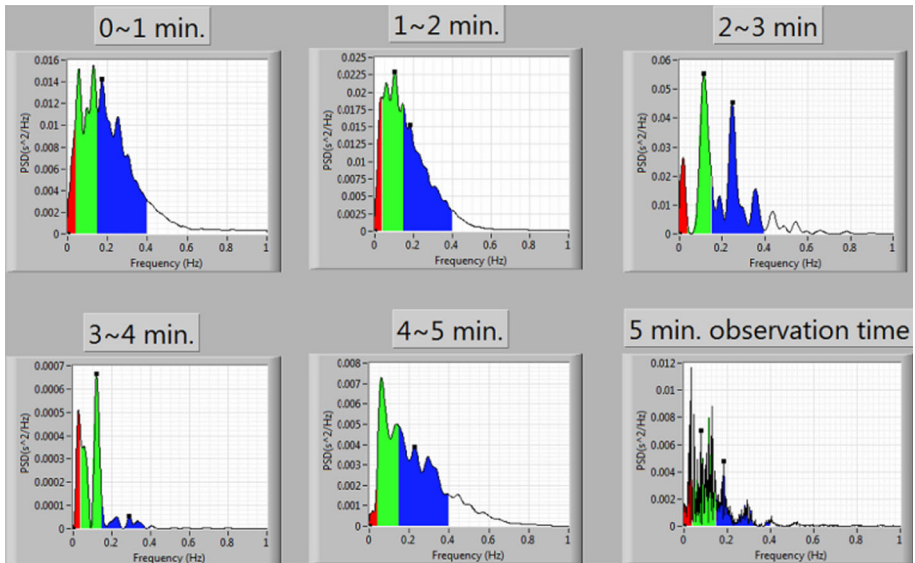


Fig. 39 Subject 4 result in static mode utilizing the FFT method

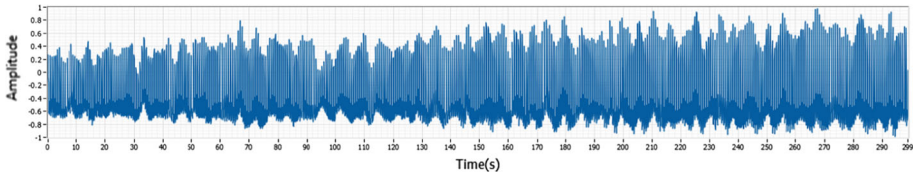


Fig. 40 Subject 5 signal in static mode

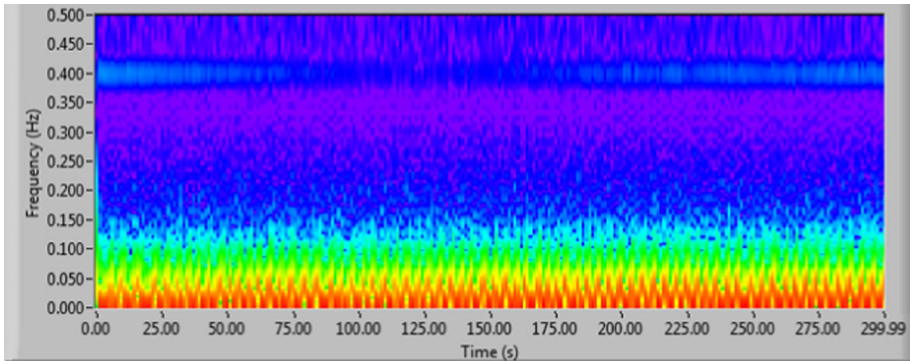


Fig. 41 Subject 5 result in static mode utilizing the STFT method

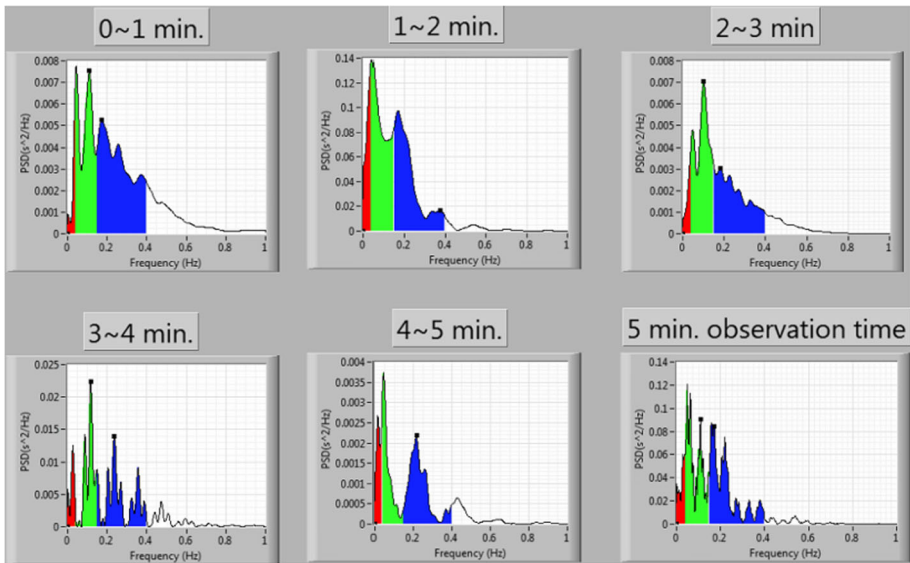


Fig. 42 Subject 5 result in static mode utilizing the FFT method

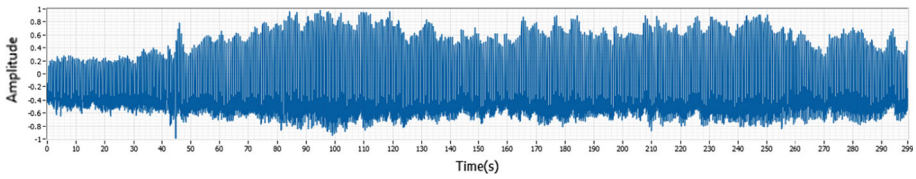


Fig. 43 Subject 6 signal in static mode

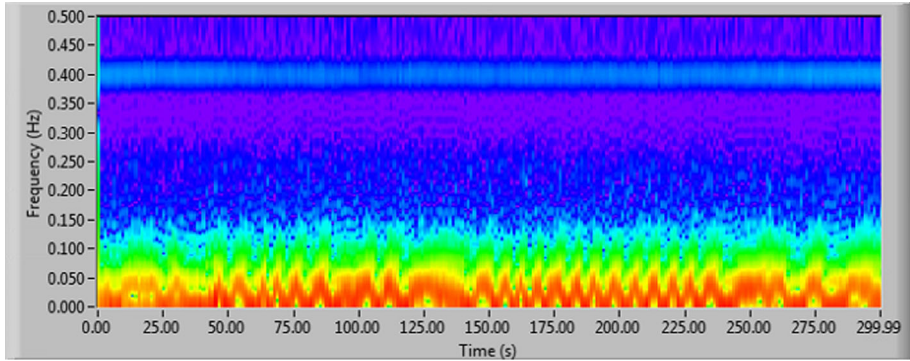


Fig. 44 Subject 6 result in static mode utilizing the STFT method

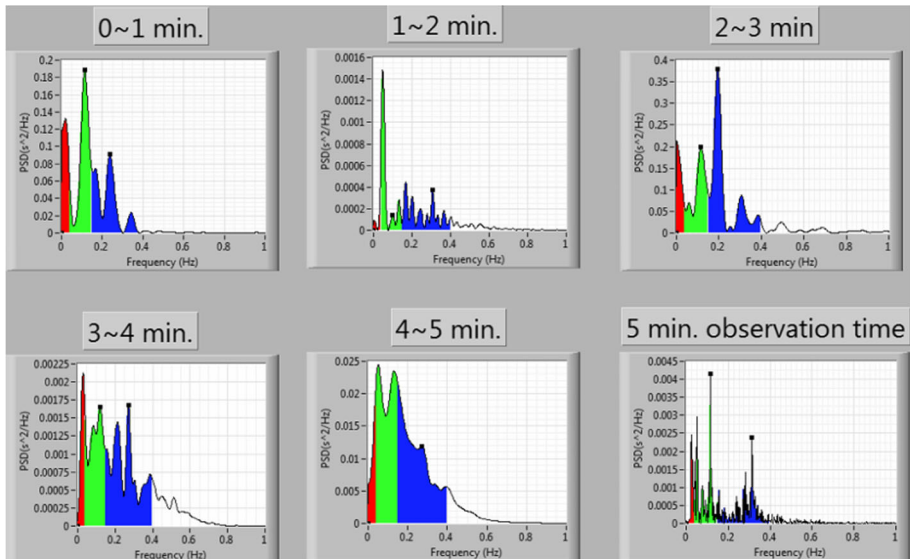


Fig. 45 Subject 6 result in static mode utilizing the FFT method

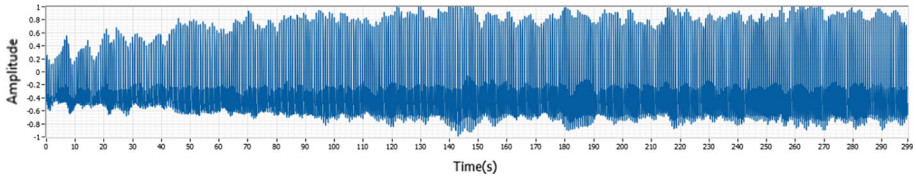


Fig. 46 Subject 7 signal in static mode

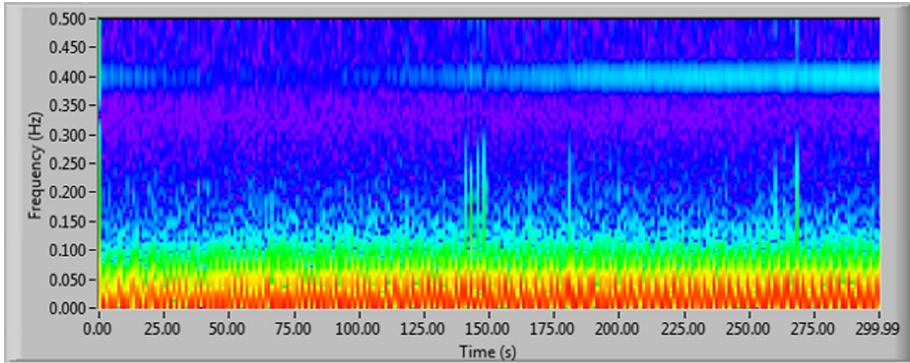


Fig. 47 Subject 7 result in static mode utilizing the STFT method

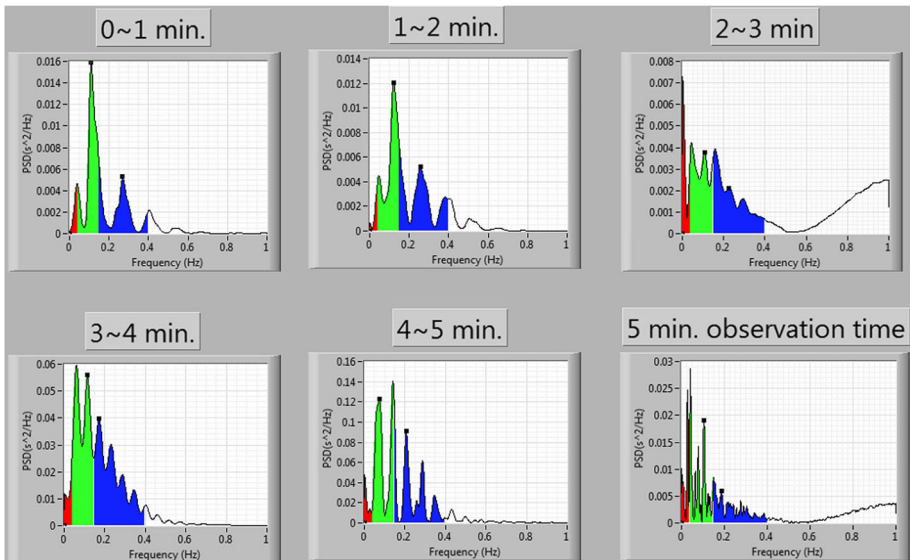


Fig. 48 Subject 7 result in static mode utilizing the FFT method

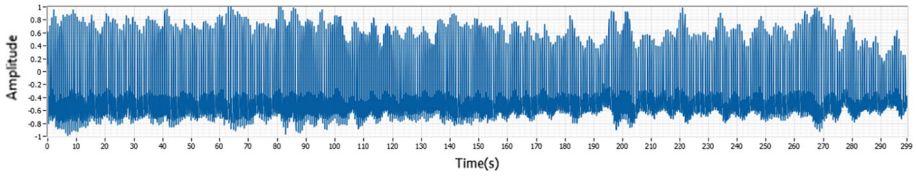


Fig. 49 Subject 8 signal in static mode

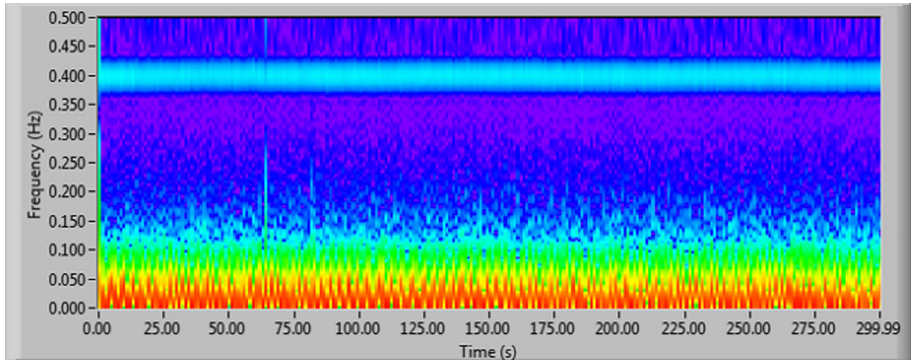


Fig. 50 Subject 8 result in static mode utilizing the STFT method

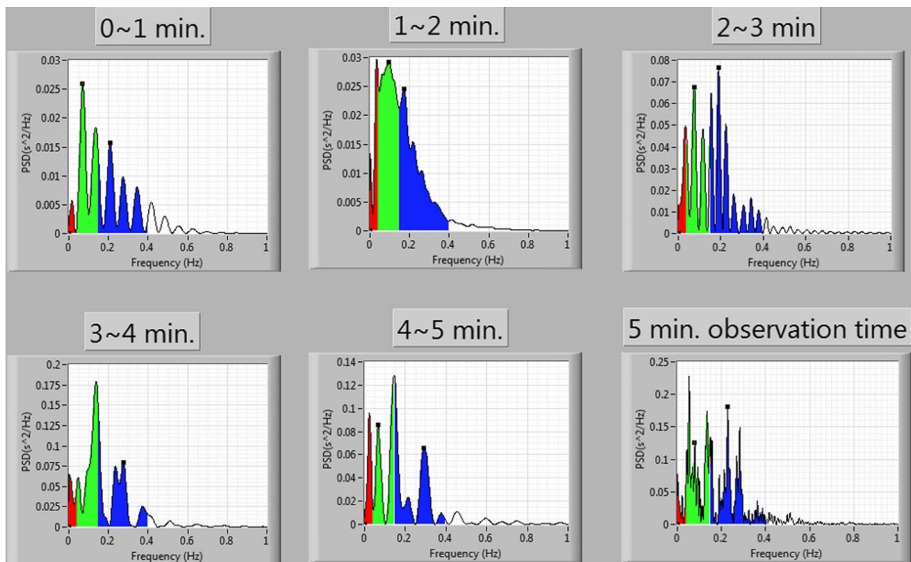


Fig. 51 Subject 8 result in static mode utilizing the FFT method

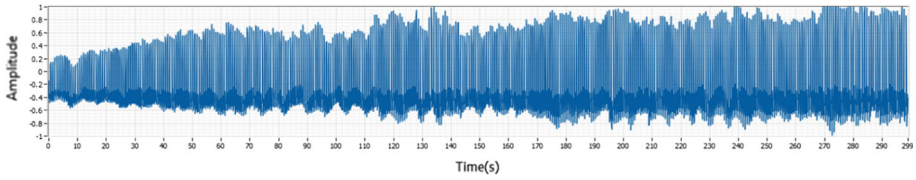


Fig. 52 Subject 9 signal in static mode

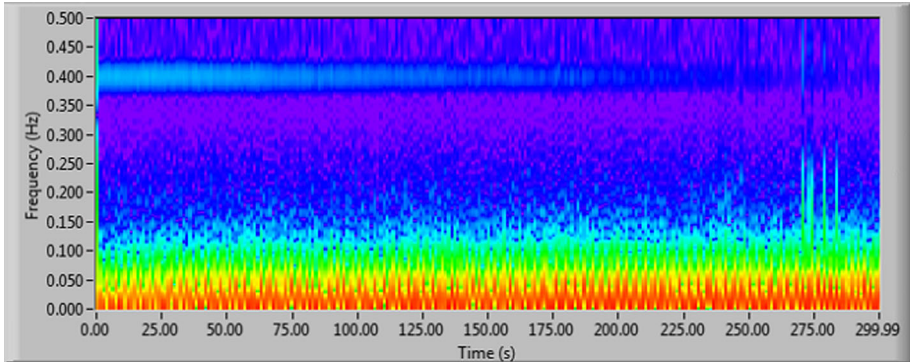


Fig. 53 Subject 9 result in static mode utilizing the STFT method

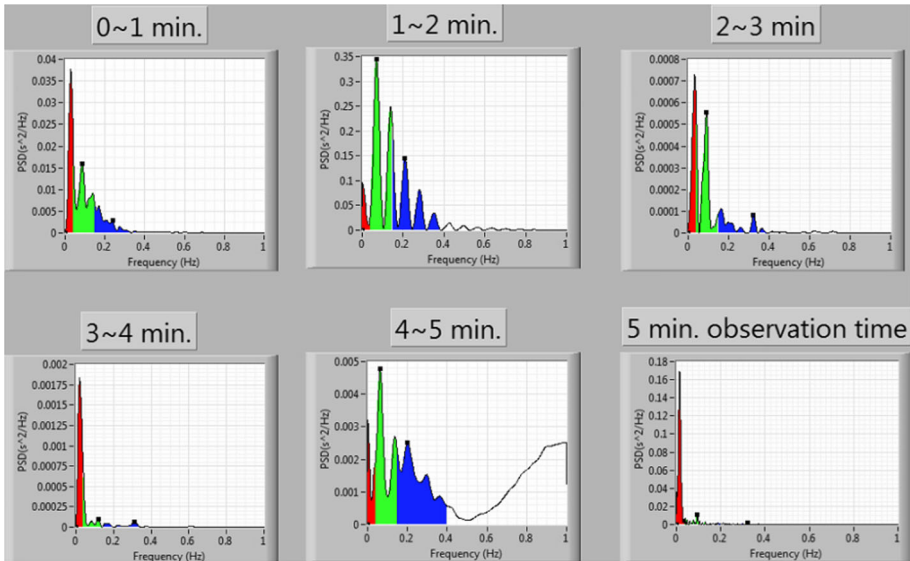


Fig. 54 Subject 9 result in static mode utilizing the FFT method

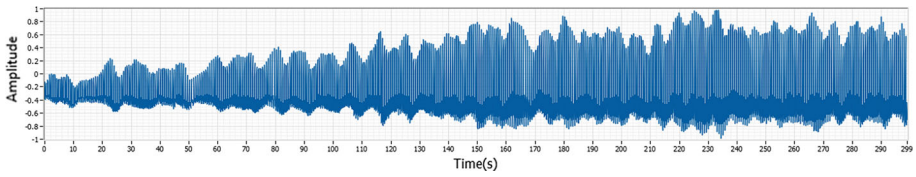


Fig. 55 Subject 10 signal in static mode

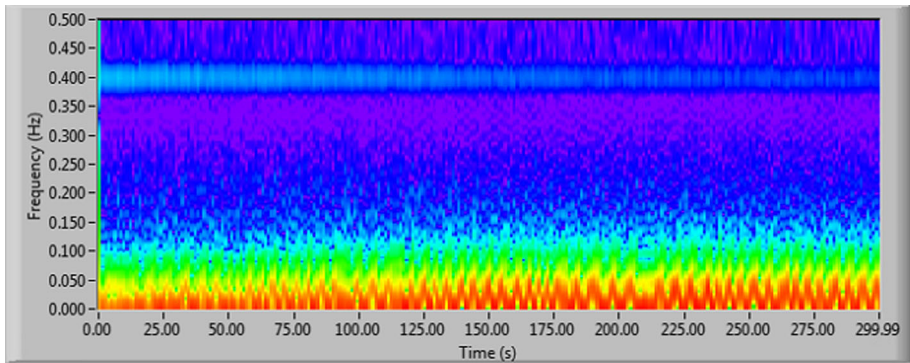


Fig. 56 Subject 10 result in static mode utilizing the STFT method

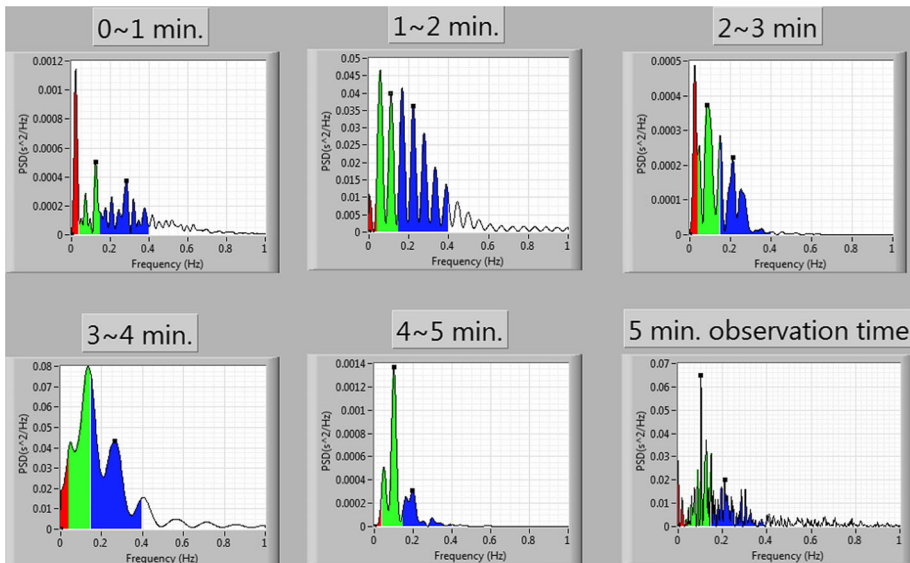


Fig. 57 Subject 10 result in static mode utilizing the FFT method

Table 8 Frequency domain results in static mode between subject 1 and subject 5

Subject	0-1			1-2			2-3			3-4			4-5		
	nLF	nHF	LF/HF	nLF	nHF	LF/HF	nLF	nHF	LF/HF	nLF	nHF	LF/HF	nLF	nHF	LF/HF
<i>Static mode</i>															
1	42.113	51.306	0.821	35.046	60.367	0.581	45.073	48.763	0.924	67.748	29.424	2.302	33.975	60.512	0.561
2	70.764	25.892	2.733	48.108	46.751	1.03	39.3	51.247	0.767	41.358	49.723	0.8318	38.657	48.063	0.804
3	48.995	43.354	1.13	52.45	37.409	1.4	73.154	24.969	2.93	57.418	40.714	1.41	49.984	39.766	1.26
4	35.48	52.517	0.675	46.45	46.925	0.99	38.988	51.04	0.764	81.948	15.646	5.238	36.531	47.525	0.769
5	32.212	48.616	0.6626	47.45	47.951	0.99	45.185	43.609	1.04	37.699	48.975	0.7698	31.937	52.196	0.612

Table 9 Frequency domain results in static mode between subject 6 and subject 10

Time period (min)	0-1			1-2			2-3			3-4			4-5		
	nLF	nHF	LF/HF	nLF	nHF	LF/HF	nLF	nHF	LF/HF	nLF	nHF	LF/HF	nLF	nHF	LF/HF
<i>Static mode</i>															
6	52.526	45.52	1.154	42.288	44.111	0.959	31.725	59.34	0.535	33.06	49.336	0.670	42.175	48.319	0.873
7	54.426	36.007	1.512	43.859	44.601	0.983	24.556	30.508	0.805	47.037	47.251	0.996	52.766	40.716	1.3
8	46.019	42.365	1.086	50.513	44.685	1.13	38.716	54.835	0.706	49.399	44.408	1.112	42.25	49.676	0.851
9	67.951	28.304	2.401	59.126	36.396	1.62	69.844	26.596	2.63	59.185	34.796	1.701	20.183	26.831	0.752
10	24.708	47.299	0.5224	32.65	53.193	0.614	55.617	42.256	1.32	40.206	47.579	0.845	69.01	29.168	2.37

Table 10 Subjects to each time period in the static mode analysis of the correlation coefficient

Time period (min)	0–1	1–2	2–3	3–4	4–5
<i>Subjects 1–10 in static mode (%)</i>					
0–1	100				
1–2	93.19	100			
2–3	82.60	90.32	100		
3–4	78.13	85.38	81.59	100	
4–5	78.40	85.93	82.99	74.26	100

Table 11 frequency domain results in static mode using FFT for 5 min

Time (min)	5 min			Time (min)	5 min		
	nLF	nHF	LF/HF		Subject	nLF	nHF
<i>Static mode</i>							
1	44.566	51.205	0.8703	6	43.564	46.415	0.9386
2	38.419	47.894	0.8022	7	32.852	27.819	1.181
3	53.058	40.987	1.295	8	45.589	47.276	0.9643
4	59.278	34.938	1.697	9	57.819	25.102	2.303
5	44.284	50.644	0.8744	10	40.975	39.101	1.048

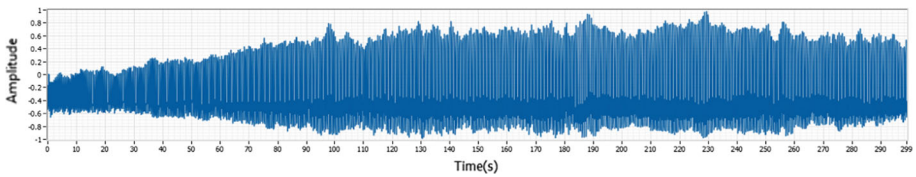


Fig. 58 Subject 1 signal in exercise mode

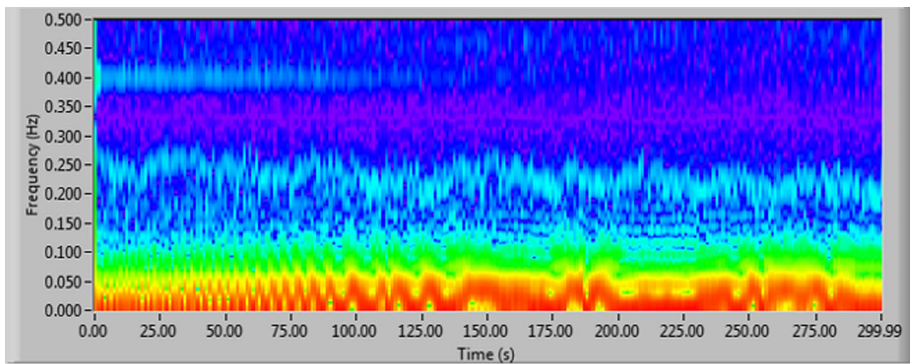


Fig. 59 Subject 1 result in exercise mode utilizing the STFT method

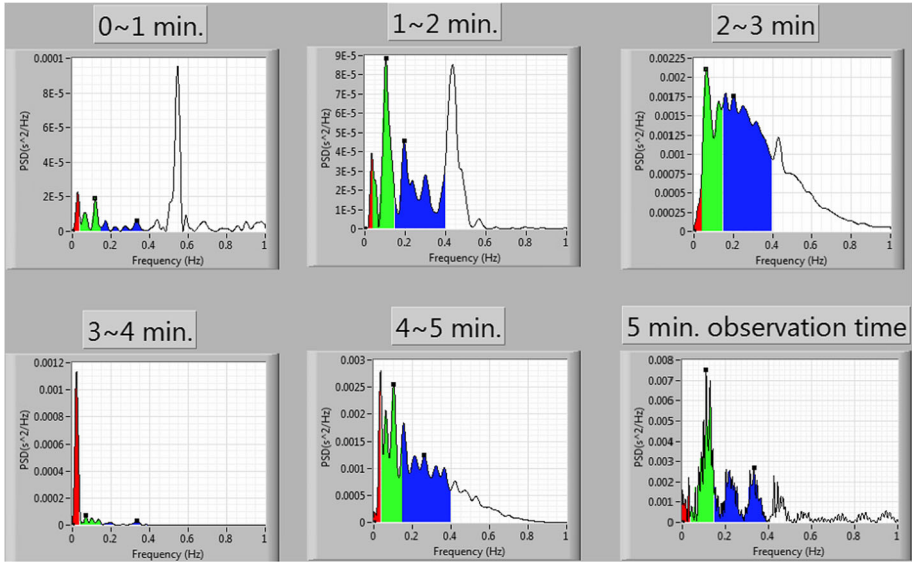


Fig. 60 Subject 1 result in exercise mode utilizing the FFT method

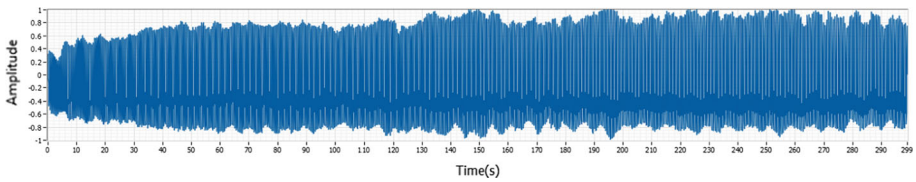


Fig. 61 Subject 2 signal in exercise mode

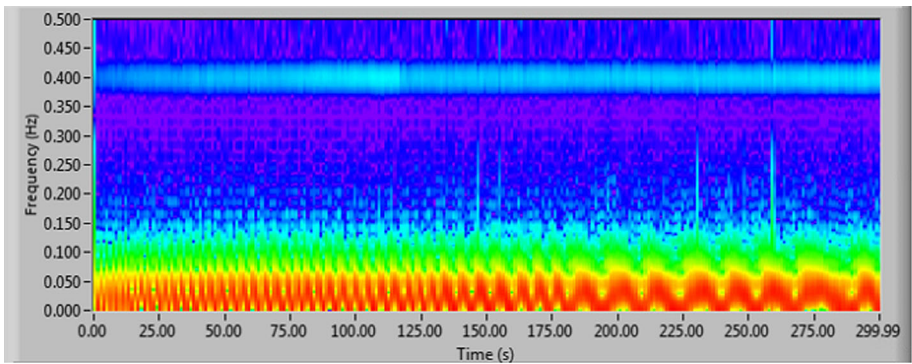


Fig. 62 Subject 2 result in exercise mode utilizing the STFT method

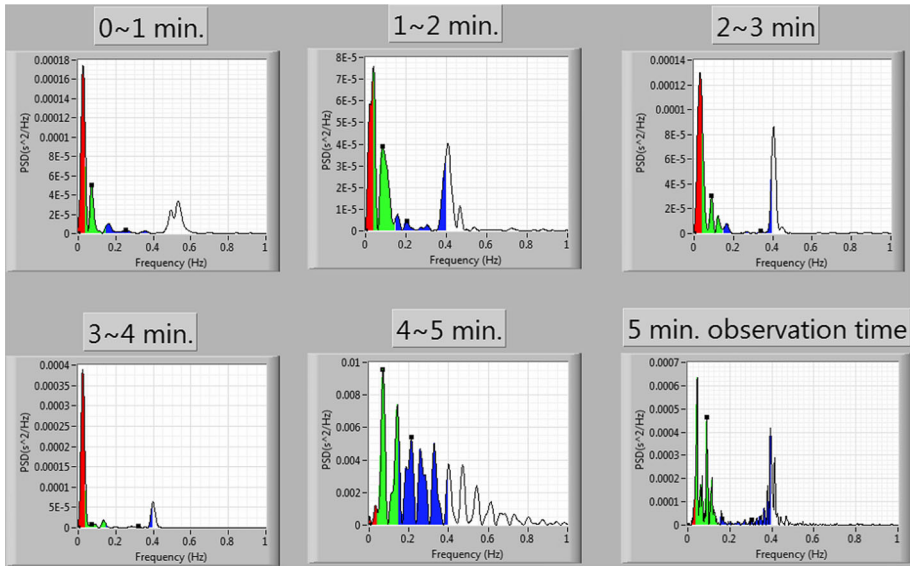


Fig. 63 Subject 2 result in exercise mode utilizing the FFT method

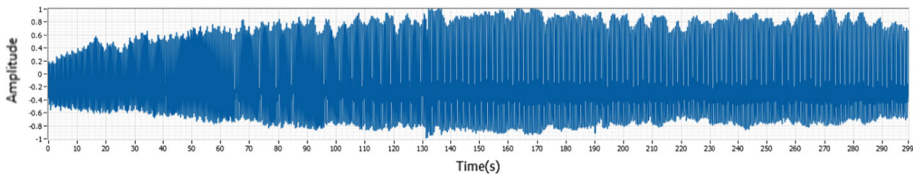


Fig. 64 Subject 3 signal in exercise mode

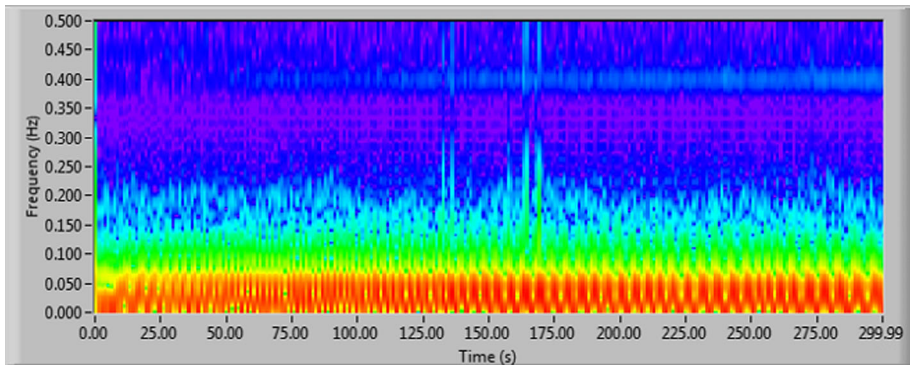


Fig. 65 Subject 3 result in exercise mode utilizing the STFT method

4.4 Exercise Mode Time Domain Analysis Results

The exercise mode is started by spinning for 5 min, and then sits on chair. While sitting, the data is recorded for 5 min. In exercise mode, the data recorded 10 times (Figs. 58, 59,

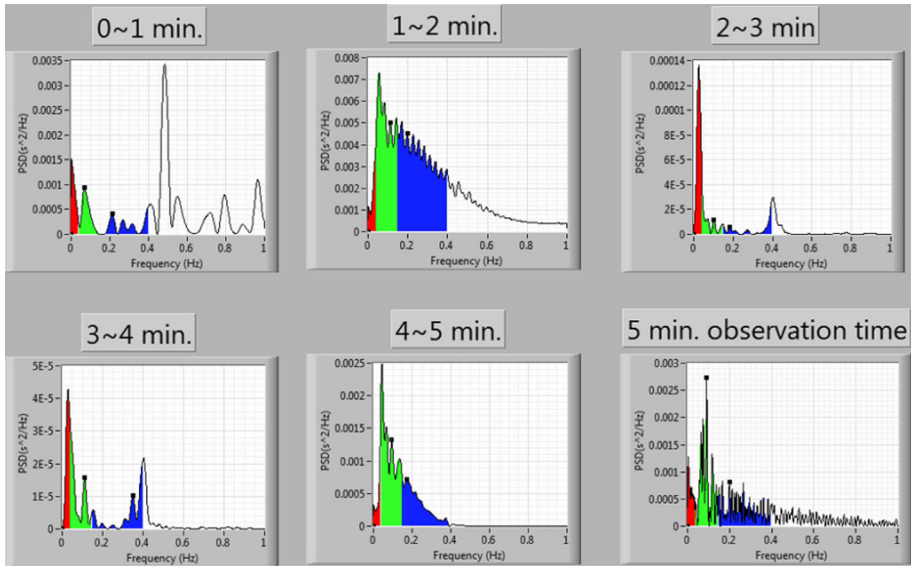


Fig. 66 Subject 3 result in exercise mode utilizing the FFT method

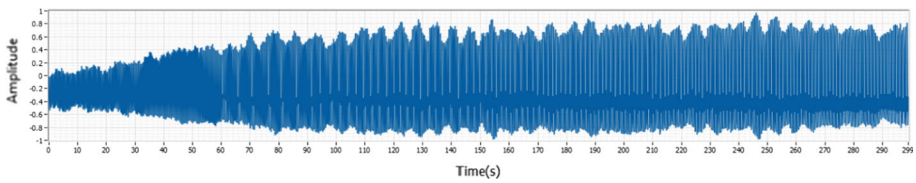


Fig. 67 Subject 4 signal in exercise mode

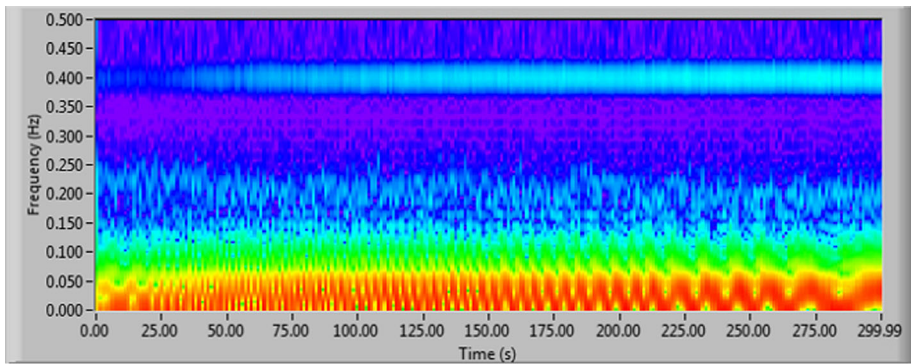


Fig. 68 Subject 4 result in exercise mode utilizing the STFT method

60, 61, 62, 63, 64, 65, 66, 67, 68, 69, 70, 71, 72, 73, 74, 75, 76, 77, 78, 79, 80, 81, 82, 83, 84, 85, 86). The subject is the author himself. The results of time domain analysis for exercise mode are shown Table 12.

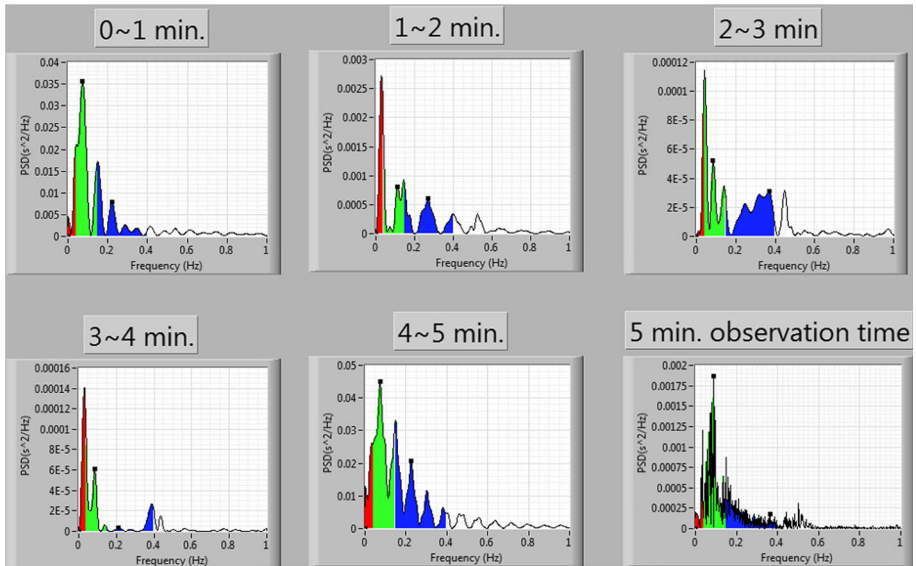


Fig. 69 Subject 4 result in exercise mode utilizing the FFT method

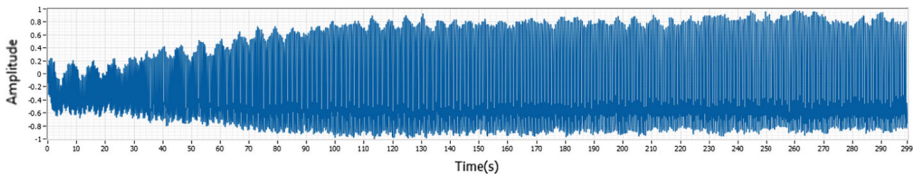


Fig. 70 Subject 5 signal in exercise mode

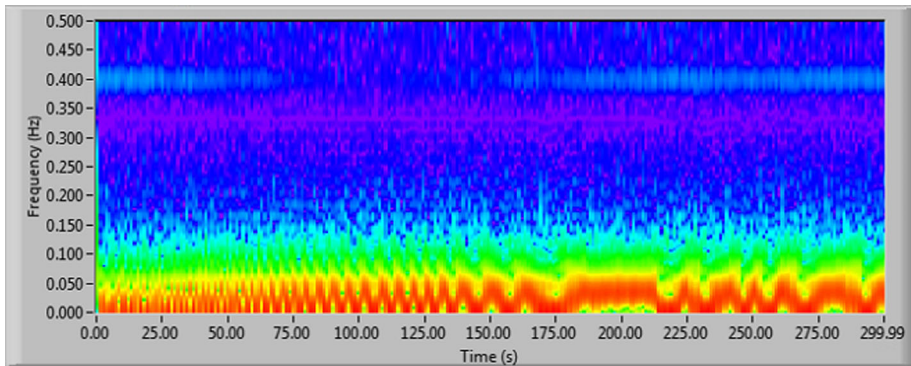


Fig. 71 Subject 5 result in exercise mode utilizing the STFT method

4.5 Exercise Mode Frequency Domain Analysis Results

Between Figs. 58 and 87 are frequency domain results in exercise mode. We recorded the waveform of frequency domain analysis, also recorded results shown in Tables 13 and 14.

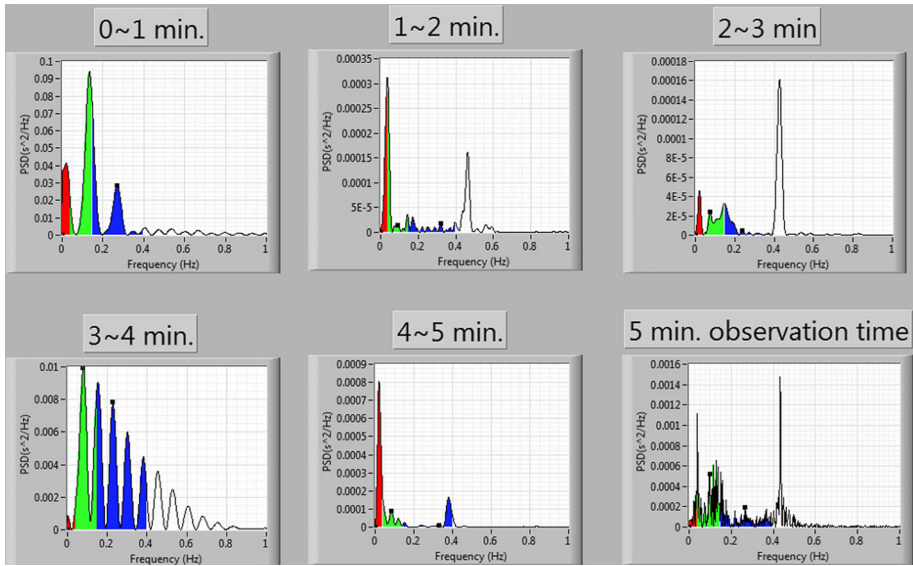


Fig. 72 Subject 5 result in exercise mode utilizing the FFT method

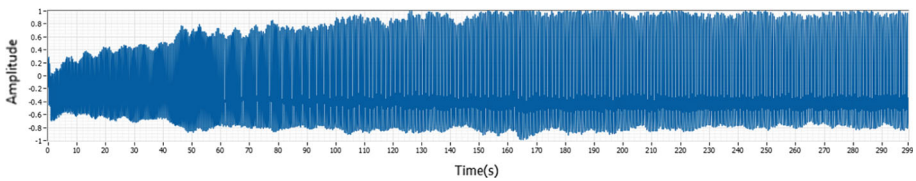


Fig. 73 Subject 6 signal in exercise mode

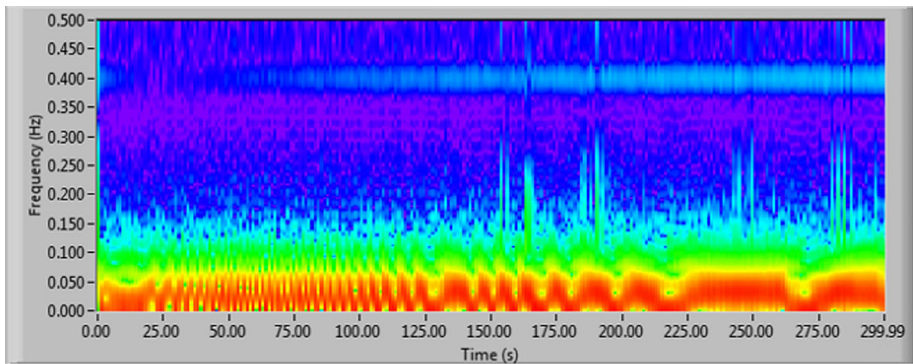


Fig. 74 Subject 6 result in exercise mode utilizing the STFT method

Tables 13 and 14 shows the recorded nLF, nHF and LF/HF for static mode. Time period was divided into 5 groups: 0–1, 1–2, 2–3, 3–4, and 4–5 (Table 15). In addition, the data derived from 5 subjects; namely subject 1 to subject 5. Table 14 shows the nLF, nHF and

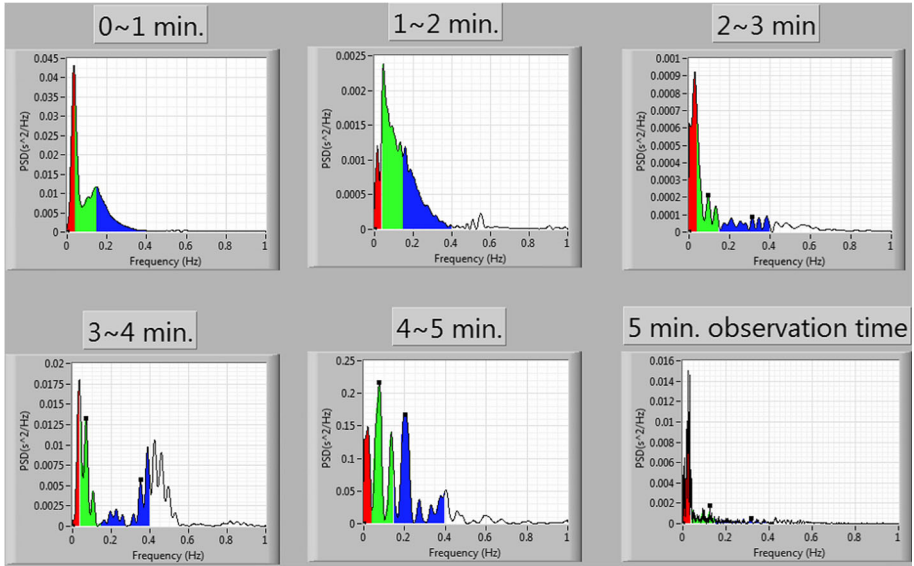


Fig. 75 Subject 6 result in exercise mode utilizing the FFT method

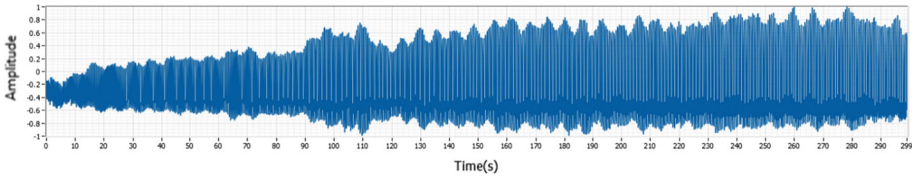


Fig. 76 Subject 7 signal in exercise mode

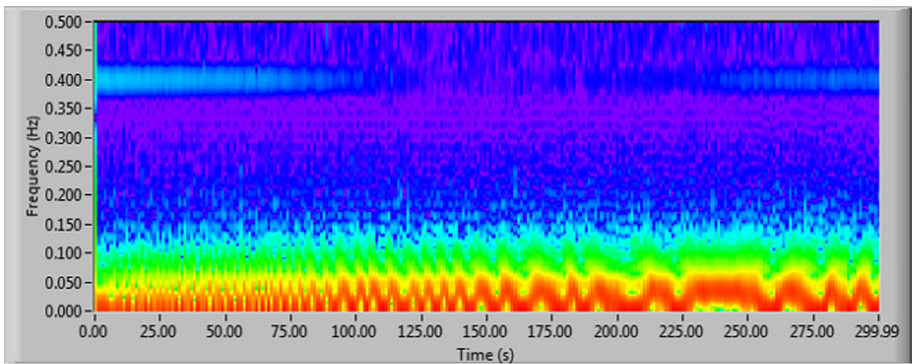


Fig. 77 Subject 7 result in exercise mode utilizing the STFT method

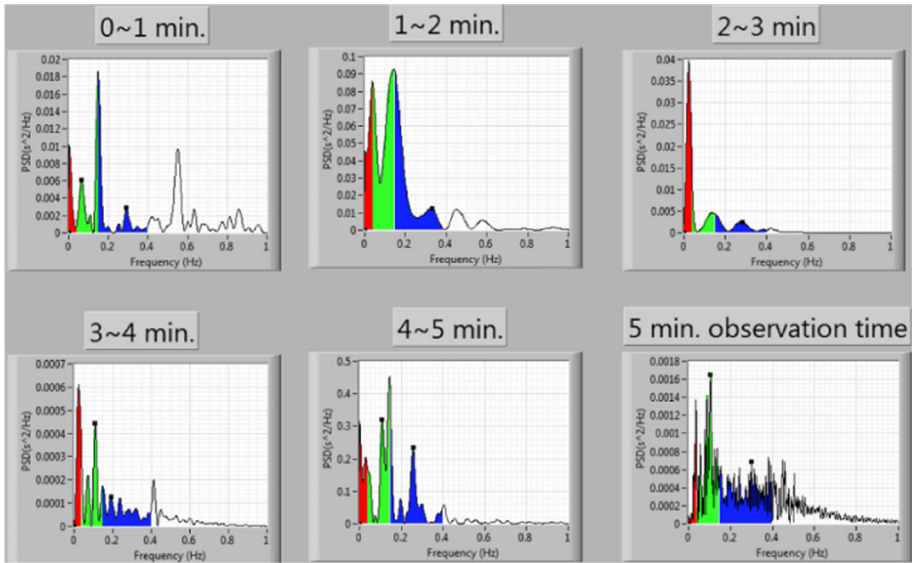


Fig. 78 Subject 7 result in exercise mode utilizing the FFT method

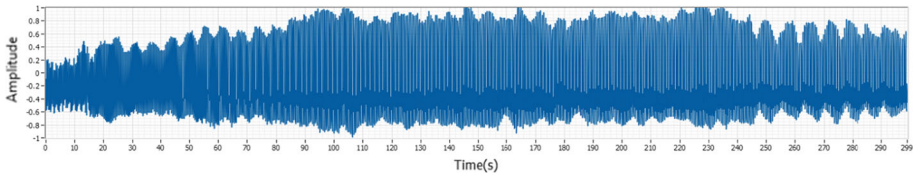


Fig. 79 Subject 8 signal in exercise mode

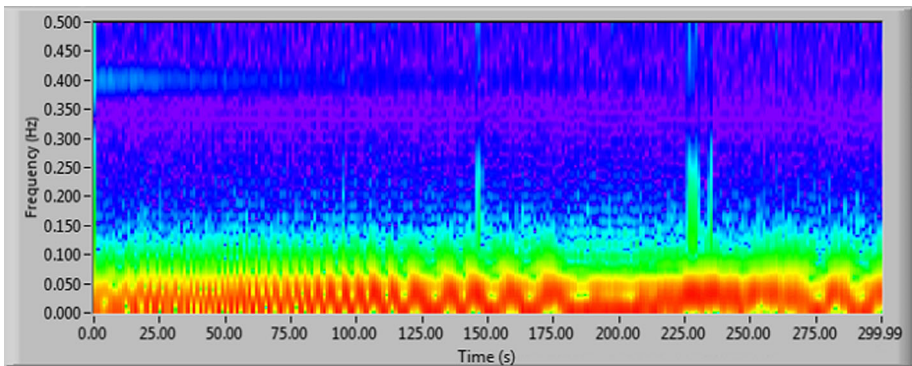


Fig. 80 Subject 8 result in exercise mode utilizing the STFT method

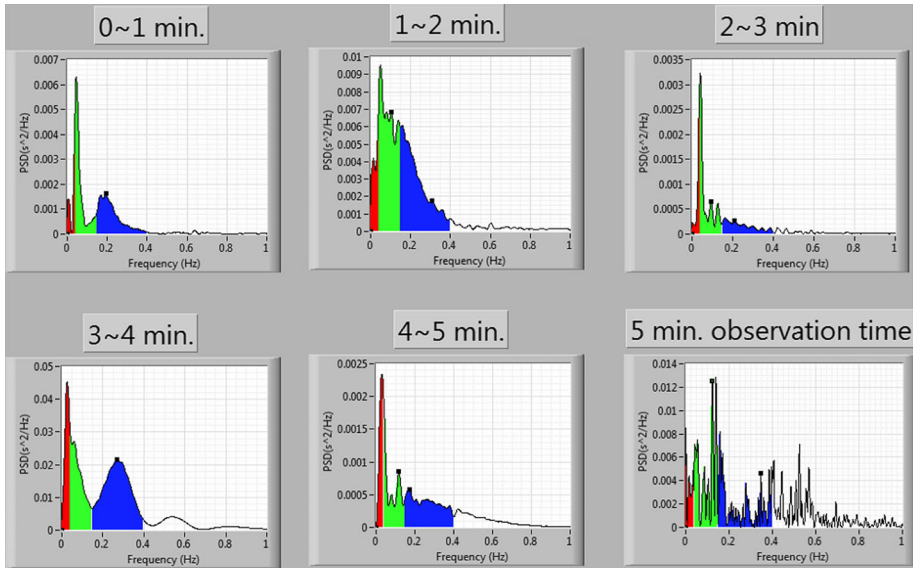


Fig. 81 Subject 8 result in exercise mode utilizing the FFT method

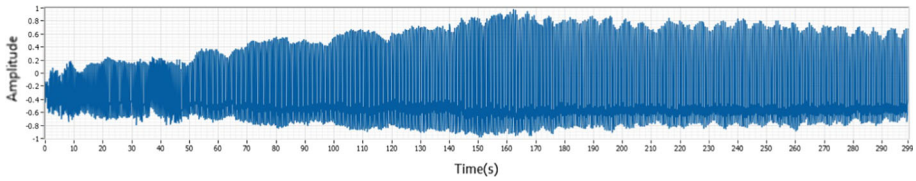


Fig. 82 Subject 9 signal in exercise mode

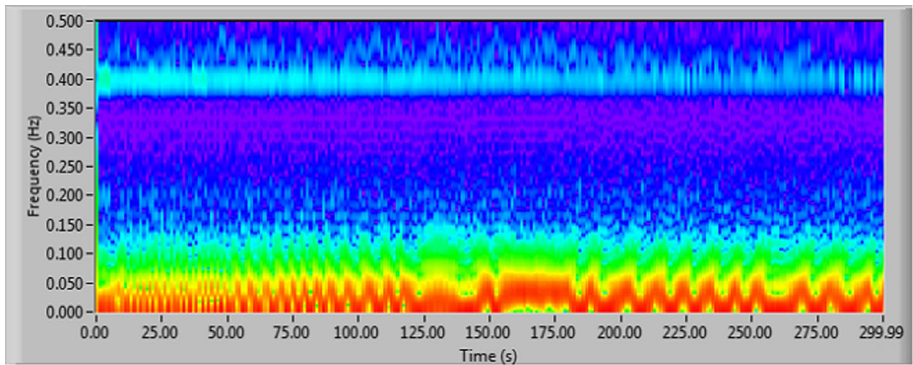


Fig. 83 Subject 9 result in exercise mode utilizing the STFT method

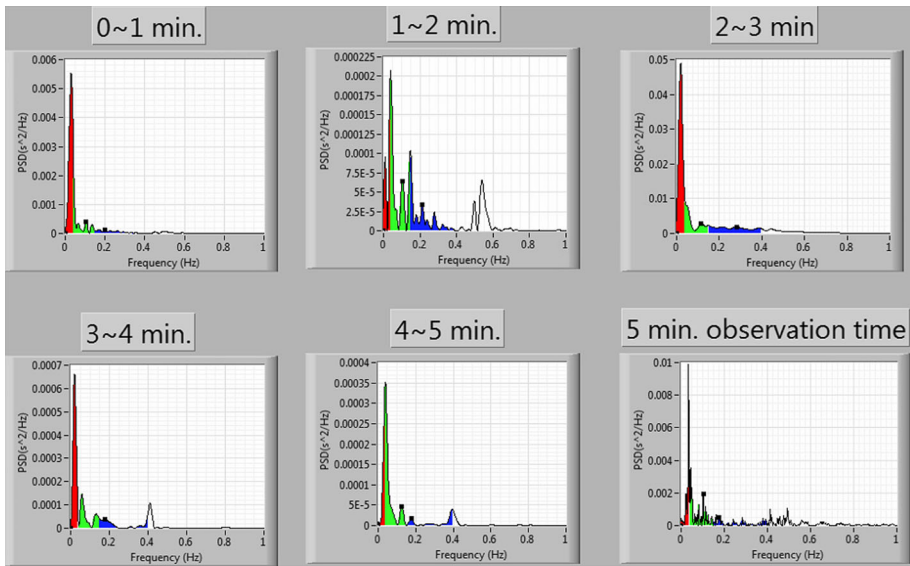


Fig. 84 Subject 9 result in exercise mode utilizing the FFT method

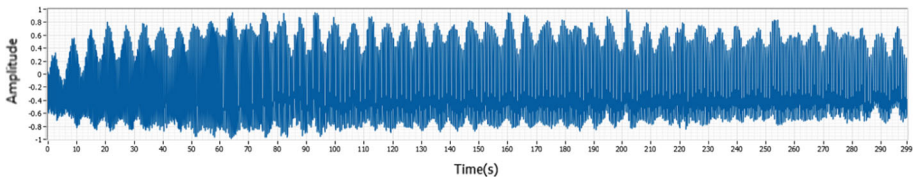


Fig. 85 Subject 10 signal in exercise mode

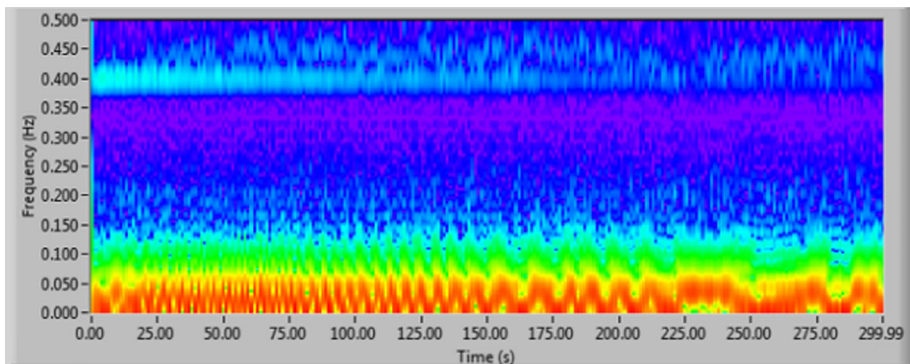


Fig. 86 Subject 10 result in exercise mode utilizing the STFT method

Table 12 Time domain results in exercise mode

Time period (min)	0–1	1–2	2–3	3–4	4–5	0–5		
Subjects	HR (bpm)	HR (bpm)	HR (bpm)	HR (bpm)	HR (bpm)	SDNN (ms)	NN50 (count)	pNN50 (%)
<i>Exercise mode</i>								
1	127	119	112	105	101	22.79	1	0.216
2	121	115	111	106	105	21.39	1	0.18
3	133	121	118	113	101	18.76	1	0.176
4	135	122	115	109	105	20.54	1	0.171
5	129	113	107	100	98	18.42	1	0.183
6	131	125	119	101	95	19.48	2	0.341
7	124	111	110	106	101	23.45	1	0.174
8	131	124	117	101	98	17.62	2	0.332
9	127	115	103	93	91	20.71	1	0.153
10	139	116	108	106	100	19.18	2	0.353

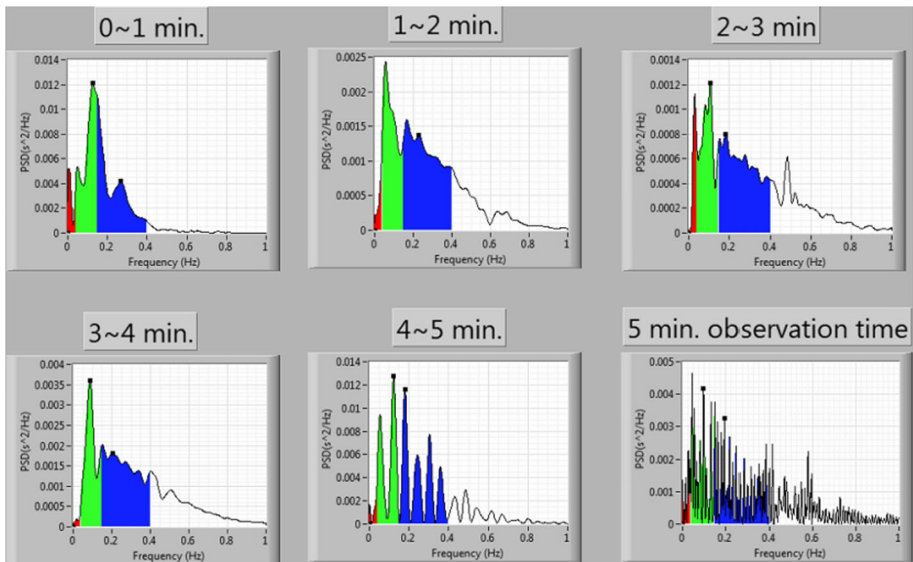


Fig. 87 Subject 10 result in exercise mode utilizing the FFT method

LF/HF values for subject 6 to subject 10. In Table 16, the FFT is used to transform the 5 min recorded PPG signals. This effort is used to compare each recorded signal.

4.6 Analysis Results in Static and Exercise Modes

For simply analysis, we collected ten subjects’ raw data in static and exercise mode. The data included mean, SD and coefficient of variation (C.V.) shown as Tables 17 and 18.

Table 13 Frequency domain results in exercise mode between subject 1 and subject 5

Subject	0-1			1-2			2-3			3-4			4-5		
	nLF	nHF	LF/HF	nLF	nHF	LF/HF	nLF	nHF	LF/HF	nLF	nHF	LF/HF	nLF	nHF	LF/HF
<i>Exercise mode</i>															
1	13.973	9.611	1.454	28.314	34	0.833	23.114	47.781	0.484	61.207	35.256	1.736	31.169	46.373	0.672
2	36.645	13.836	2.649	49.292	21.607	2.28	39.853	22.416	1.78	37.064	35.311	1.05	29.79	44.263	0.673
3	11.166	10.507	1.063	28.64	44.666	0.641	34.409	31.685	1.09	41.509	35.25	1.178	61.915	37.165	1.67
4	60.272	25.217	2.391	33.629	41.205	0.816	35.674	45.104	0.791	55.542	25.024	2.22	49.931	37.452	1.33
5	53.331	37.16	1.435	32.296	18.054	1.79	22.166	16.772	1.32	31.479	48.539	0.649	42.974	48.68	0.883

Table 14 Frequency domain results in exercise mode between Subject 6 and Subject 10

Subject	0-1			1-2			2-3			3-4			4-5		
	nLF	nHF	LF/HF	nLF	nHF	LF/HF	nLF	nHF	LF/HF	nLF	nHF	LF/HF	nLF	nHF	LF/HF
<i>Exercise mode</i>															
6	56.311	36.787	1.531	57.177	35.866	1.59	44.787	29.387	1.52	29.293	27.389	1.07	43.509	44.323	0.982
7	28.049	23.239	1.207	52.08	37.113	1.4	40.573	48.694	0.833	35.417	36.328	0.975	50.747	39.868	1.27
8	47.535	46.801	1.016	47.65	44.134	1.08	55.564	31.939	1.74	29.932	55.627	0.5381	30.714	44.72	0.687
9	65.975	23.271	2.835	46.522	25.061	1.86	36.995	41.295	0.896	47.59	29.385	1.62	70.98	19.25	3.69
10	46.577	48.896	0.953	29.488	47.566	0.62	26.339	44.055	0.598	25.879	43.361	0.597	33.914	47.899	0.708

Table 15 Subjects to each time period in the exercise mode analysis of the correlation coefficient

Time period (min)	0–1	1–2	2–3	3–4	4–5
<i>Subjects 1–10 in exercise mode (%)</i>					
0–1	100				
1–2	77.43	100			
2–3	67.30	92.36	100		
3–4	69.43	77.77	74.19	100	
4–5	74.18	82.92	78.59	87.77	100

Table 16 frequency domain results in exercise mode using FFT

Time (min)			Time (min)				
5 min			5 min				
Subject	nLF	nHF	LF/HF	Subject	nLF	nHF	LF/HF
<i>Exercise mode</i>							
1	40.303	38.007	1.06	6	42.052	30.432	1.382
2	51.074	29.597	1.726	7	29.702	38.649	0.769
3	36.545	34.106	1.072	8	33.296	30.181	1.103
4	54.562	31.48	1.733	9	42.87	19.993	2.144
5	36.478	28.161	1.295	10	26.74	39.099	0.684

Table 17 Mean, SD, and C.V. parameters of raw data in static mode

Subject	Mean ± SD (mV)	C.V. (%)
<i>Raw data in static mode</i>		
1	7.72 ± 2.32	30.05
2	7.73 ± 2.16	28.01
3	7.74 ± 1.07	13.82
4	7.73 ± 1.54	19.95
5	7.73 ± 1.64	21.25
6	7.72 ± 1.96	25.44
7	7.72 ± 2.35	30.37
8	7.71 ± 2.16	28.04
9	7.72 ± 2.17	28.06
10	7.72 ± 1.81	23.48

Table 18 Mean, SD, and C.V. parameters of raw data in exercise mode

Subject	Mean \pm SD (mV)	C.V. (%)
<i>Raw data in exercise mode</i>		
1	7.71 \pm 0.95	12.36
2	7.72 \pm 2.76	35.76
3	7.71 \pm 2.65	34.45
4	7.70 \pm 2.21	28.70
5	7.71 \pm 1.98	25.63
6	7.69 \pm 2.83	36.80
7	7.69 \pm 2.16	28.06
8	7.70 \pm 2.53	32.87
9	7.71 \pm 2.01	26.08
10	7.71 \pm 2.03	26.34

5 Conclusions

In this paper, in order to capture physiological signals in static and exercise modes using the green LED reflective PPG are done for ten times. The measuring time is 5 min. The measured data cuts into five segments for time domain and frequency domain analysis through STFT. Then, we find the physiological significance of each representative signal.

According to the experimental results in time domain analysis, the value of SDNN is about 25.95 ms and the average heartbeat is about 91.32 bpm in the static mode. Meanwhile, the value of SDNN is about 20.23 ms. The average heartbeat is about 112.66 bpm in the exercise mode. Moreover, the value of LF/HF in time frequency analysis is about 1.22 in static mode. The value of LF/HF is about 1.29 in the exercise mode. Refer to Tables 17 and 18 for static mode and exercise mode, the raw signals in static mode C.V. is about 24.85%; and for the exercise mode, C.V. is about 28.71%. Those shows that the signals in the exercise mode are vary larger than the static mode.

Furthermore, according to the static and exercise mode frequency domain results per minute correlation coefficient analysis, the correlation coefficient of static mode is about 80%, and the correlation coefficient of exercise mode is about 70%. In the correlation coefficient for 2–3 min with 0–1 min of the exercise mode falls below 0.7, and the reason for the state to exercise condition back to the static condition of measurement, thus, physiological condition stabilized.

In the hardware, PPG equipment is suffered from body shaking during measurement. Since the contact position is not good, the data is inaccurate. In static mode measurement and record signal is easier than in exercise mode; therefore, the combination of green and infrared light reflective PPG in the future, and enhance its stability, practicality, and correlation analysis between SpO₂ and autonomic nerve system.

In terms of data, due to only take their own experiments results to make inferences, the number of samples is too small. We will increase the number of data samples and different ages in the future, and brought together into big data. We believe the data which in the statistical analysis would be more accurate and reliability also would higher. In the application of future, we can explore emotional management in the case of listening music by this paper method, then through various emotional states, to observer correlation between different physiological states and HRV. And sort out the correlation statistical results, for further analysis.

References

1. Fu, T.-H. (2010). Application of time–frequency analysis of infrared plethysmograph waveform. *International Journal of Advanced Information Technologies*, 4(6), 105–118.
2. Weng, K.-P., Ho, T.-Y., Ou, S.-F., Lin, C.-C., & Hsieh, K.-S. (2009). Analysis of heart rate variability. *Taiwan Medical Journal*, 52(6), 12–13.
3. Liu, S.-H., Chang, K.-M., & Fu, T.-H. (2010). Heart rate extraction from photoplethysmogram on fuzzy logic discriminator. *Journal of Engineering Applications of Artificial Intelligence*, 23(9), 968–977.
4. Li, X.-E., Fang, J.-C., & Li, Y.-D. (2009). *Measurement and analysis of PPG signal* (pp. 4–7). Taichung: Feng Chia University.
5. Pulse Sensor V4.4. <http://share.eepw.com.cn/share/download/id/382273>.
6. Appel, L. J., Brands, M. W., Daniels, S. R., Karanja, N., Elmer, P. J., & Sacks, F. M. (2006). Dietary approaches to prevent and treat hypertension: a scientific statement from the American Heart Association. *Hypertension*, 47, 296.
7. Boundless. Introduction to Blood Pressure. *Boundless Anatomy and Physiology*. Boundless, 21 July 2016. Retrieved 27 Jan 2016.
8. Blood Pressure UK. <http://www.bloodpressureuk.org/>.
9. Datasheet of AM2520ZGC09. <https://www.kingbrightusa.com/images/catalog/spec/AM2520ZGC09.pdf>.
10. Datasheet of APSD-9008. <http://www.avagotech.com/docs/AV02-1169EN>.
11. Datasheet of MCP6001. <http://ww1.microchip.com/downloads/en/devicedoc/21733j.pdf>.
12. Guyomard, J., & Stortelder, R. (2015). *Heart rate measurement through PPG: Heartbeat measurement in a wireless headset* (pp. 5–6). Delft: The Delft University of Technology.
13. LabVIEW STFT Spectrograms VI. http://zone.ni.com/reference/en-XX/help/371361J-01/ivanls/stft_spectrogram_core/.
14. Liangfang, Y.I.N., Yuanqing, X.I.A.O., Zhenyu, X.U. (2013). A new principle based on Pearson correlation coefficient to avoid mal-operation of the restricted earth fault protection. In *22nd international conference on electricity distribution Stockholm*.
15. Malik, M. (1996). Heart rate variability. *European Heart Journal*, 444, 354–381.
16. Kautzner, J. (1995). Reproducibility of heart rate variability measurement. In M. Malik & A. J. Camm (Eds.), *Heart rate variability* (pp. 165–171). Armonk: Futura Publishing Co., Inc.
17. Kamath, M. V., Watanabe, M. A., & Upton, A. R. M. (2011). Heart rate variability: A historical perspective. Department of Physiology and Cell Biology, the Ohio State University Columbus, OH, USA. *Frontiers in Physiology*, 2(86), 86. doi:10.3389/fphys.2011.00086.
18. Mayo Clinic. <http://www.mayoclinic.org/>.
19. MEDICORE. Heart rate variability analysis system. http://medi-core.com/download/HRV_clinical_manual_ver3.0.pdf. Accessed 16 March 2015.
20. Moissl, U., Garzotto, F., Signorini, M. G., Cruz, D., Tetta, C., Ronco, C., Gatti, E., & Cerutti, S. (2010). Study of the autonomic response in hemodialysis patients with different fluid overload levels. In *Annual international conference of the IEEE, engineering in medicine and biology society (EMBC)* (pp. 3796–3799).
21. Pearson correlation coefficient. https://zh.wikipedia.org/wiki/Pearson_product-moment_correlation_coefficient.
22. Peng, R.-C., Zhou, X.-L., Lin, W.-H., & Zhang, Y.-T. (2015). Extraction of heart rate variability from smartphone photoplethysmograms. *Computational and Mathematical Methods in Medicine*, 2015, 11. (Article ID 516826).
23. Samuel & Mueller, D. The circulatory system. <http://carignanapbio.weebly.com/circulatorysystem.html>.
24. Schwa, P. J., & Stone, H. L. (1982). The role of the autonomic nervous system in sudden coronary death. *Annals of the New York Academy of Sciences*, 382, 162–180.
25. Systolic & Diastolic Blood Pressure. <http://www.diffen.com/>.



Gwo-Jia Jong received a B.S. degree in electronic engineering from National Taiwan University of Science and Technology, Taiwan, 1984, and Ph.D. degree in Electric engineering from Paisley University, United Kingdom, 2000. In 2002 he joined the faculty of National Kaohsiung University of Applied Sciences, Taiwan where he is currently a professor in Department of Electronic Engineering. He is currently also an adjunct professor in Institute of Clinical Medicine, Kaohsiung Medical University. His research interests include Electronic Engineering, Communication Engineering, Digital and Wireless Communication systems, and Biomedical System Integration. He is also a team project leader of Center for Electronic Communication Technology (CECT) of Ministry of Education in Taiwan.



Aripriharta received his S.T. (2004) and M.T. (2012) in Electrical Engineering from Brawijaya University, Indonesia. Since 2005, he joined the Faculty of Engineering, State University of Malang Indonesia as Lecturer and Research Leader in Power Electronics and Drives Laboratories. He is a Member of IAENG. He is currently a PhD Student in National Kaohsiung University of Applied Sciences, Taiwan. His interest is intelligent system and its applications.



Gwo-Jiun Horng received an M.S. (2008) in electronic engineering from National Kaohsiung University of Applied Sciences, Kaohsiung, Taiwan. He is received the Ph.D. (2013) in Computer Science and Information Engineering at National Cheng Kung University, Taiwan. He is currently an assistant professor in the Department of Computer Science and Information Engineering, Southern Taiwan University of Science and Technology, Tainan, Taiwan. His research interests include mobile service and computing, adaptive systems, intelligent information systems, wireless/vehicle networks and communications.